

# Feasibility of thorium extraction from a solid monazite matrix utilizing supercritical CO<sub>2</sub> with TBP and HFA as chelates

**B de C Mastoroudes**  
**20383576**

Dissertation submitted in *partial* fulfillment of the  
requirements for the degree *Magister Engeneriae* in  
Mechanical Engineering at the Potchefstroom Campus of  
the North-West University

Supervisor: Prof J. Markgraaff

November 2014

# Acknowledgements

I would like to thank the following persons for their continued support throughout this work without them this study would surely not have been a success.

**All honour and glory to God**

My parents and girlfriend for all the love and support during my studies.

My study leader Prof J. Markgraaff whose guidance was instrumental to this project.

The South African Nuclear Energy Corporation for all the analyses.

The North-West University.

My dear friend A. Els for his personal input.

## Abstract

With current energy demands globally and locally, nuclear energy remains one of the top competitors for cleaner and sustainable energy. The nuclear industry requires more inherent safety and proliferation resistance in reactor design. Thorium has therefore been identified as a possible fuel for future nuclear reactors that can comply with these requirements. However current extraction techniques are expensive, time consuming and generate large quantities of hazardous waste. A possible alternative to conventional solvent extraction of thorium is SFE (Supercritical Fluid Extraction).

A monazite sample from the Steenkampskraal mine was investigated using SEM (Scanning Electron Microscope) analysis methods to determine the distribution of thorium in the grains that could potentially complicate the effectiveness of the SFE extraction method if zoning is present. The results show a homogeneous distribution with no discernable zonation in the grains. The concentration of Th, Ce and Nd was determined by quantitative MPA (Micro Probe Analysis). The results obtained from the MPA point analysis on several grains show average Th, Ce and Nd concentrations of 6.5 wt. %, 24.1 wt. % and 9.7 wt. % respectively.

The extraction of  $\text{Th}^{+4}$  from a filter paper was conducted to verify the extraction procedure and extractability of transition elements employing SFE. The extraction was conducted using supercritical  $\text{CO}_2$  and methanol as co-solvent with TBP (Tributyl Phosphate) and HFA (Hexafluoroacetylacetone) added *in situ* as chelates. ICP-MS results for the  $\text{Th}^{+4}$  extraction procedure showed extraction efficiency of 53 % compared to 83 % in literature (Kumar *et al.* 2009). This marked difference in extraction efficiency is attributed to ineffective trapping methods employed and lack of prior maintenance and support on the extraction apparatus. Subsequently all further extracted samples of Th from monazite were tested using XRF analysis methods.

Due to the lack of prior maintenance on the extraction apparatus several technical breakdowns were encountered and addressed from a mechanical engineering standpoint. The operational effectiveness of the modified apparatus was verified through the extraction of marula seed oil and compared with another supercritical fluid (SF) extractor to show 50 % extraction efficiency in each case.

A review of the literature indicated that the crystal chemical requirements for substitution of trivalent ( $\text{Ce}^{+3}$ ) for tetravalent ( $\text{Th}^{+4}$ ) may be fulfilled during SFE processes. Experimental substitution extractions were conducted by addition of different chelates and were conducted by subjecting the monazite samples to 20 MPa pressure for 180 min static flow and 10 min

continuous flow extraction times with a CO<sub>2</sub> flow rate of 2 mL/min with 10 % co-solvent flow rate. The results of the two sets of substitution extractions namely  $\alpha$  and  $\beta$  show no clear indication of Th extraction. The maximum theoretical efficiency obtainable under current extraction equipment limitations was calculated as 12%. The XRF analysis error margin was given by the analytical laboratory as 10 %.

The literature has shown the substitution of trivalent cations for tetravalent cations in the monazite structure to be a valid reaction mechanism. The experimental results showed little or no success in extracting thorium from monazite. In order to prove the practical feasibility of thorium extraction several changes to the experimental operating conditions is required.

*Keywords:*

Supercritical fluid, CO<sub>2</sub>, Chelates, Thorium, Rare earth elements, Supercritical fluid extraction, solvent extraction.

# Contents

Abstract.....	ii
1 Introduction .....	1
1.1 Problem statement .....	2
1.2 Aim .....	2
2 Literature Review .....	3
2.1 Monazite .....	3
2.2 Solvent extraction .....	6
2.3 Supercritical fluids.....	10
2.4 Supercritical Extraction .....	11
2.4.1 Liquid phase extraction.....	12
2.4.2 Extraction from a solid phase .....	12
2.5 Variables affecting SFE .....	15
2.5.1 Temperature .....	15
2.5.2 Pressure.....	15
2.5.3 Viscosity .....	16
2.5.4 Extraction time.....	16
2.5.5 Phase behaviour.....	17
2.5.6 Grain size.....	18
2.5.7 Crystal chemical parameter .....	18
2.5.8 Solubility.....	19
2.6 Solvent, chelates and modifiers.....	22
2.6.1 Solvent .....	22
2.6.2 Chelate .....	27
2.6.3 Choosing a modifier .....	31
2.6.4 Synergistic extraction.....	31
2.7 Trapping .....	32
2.8 Extraction protocol .....	33
2.9 Summary .....	34
3 Experimental work.....	35
3.1 Mineralogical characterization .....	35
3.2 Extraction equipment .....	40
3.3 SFE extraction procedure.....	41

3.4	Kumar experiment .....	43
3.5	Ce substitution extraction protocol .....	46
3.5.1	Ce <sup>+3</sup> substitution $\alpha$ -extraction procedure .....	48
3.5.2	Ce <sup>+3</sup> substitution $\beta$ extraction procedure .....	49
3.6	Ce <sup>+3</sup> Extraction validation.....	50
4	Conclusion.....	52
5	Bibliography .....	54
6	Appendix A: Extraction equipment.....	57
6.1	Major subsystems .....	57
6.1.1	Engineering and maintenance of the LECO TFE 2000™ .....	60
7	Appendix B: Data and calculations.....	63

## List of figures

Figure 1 Structural representation of a monazite polyhedral.....	4
Figure 2 Representation of a unit cell repetition of monazite .....	4
Figure 3 Phase diagram: CO <sub>2</sub> (after 1) .....	10
Figure 4: Schematic of a supercritical extraction setup.....	11
Figure 5 Representation of interaction between SFE components (after Dean. 1993).....	19
Figure 6 Parameter $\pi^*$ for solvability (Luque de Castro <i>et al.</i> 2010) .....	23
Figure 7 Structure illustration of a chelating reaction .....	27
Figure 8 Bond structure illustration of Li(FDDC) .....	28
Figure 9 Bond structure illustration of enolate formation during metal complexation .....	28
Figure 10 Bond structure illustration of crown ether .....	30
Figure 11 Photo of a polished sample of monazite grains imbedded in an epoxy resin. ....	35
Figure 12 BSE image of monazite grains with element distribution maps.....	36
Figure 13 Microprobe BSE image of monazite grains illustrating 15 analysed points. ....	37
Figure 14 LECO TFE 2000™ supercritical extraction apparatus and set-up.....	40
Figure 15 Exploded view of the sample holder assembly including a funnel.....	41
Figure 16 NATEX SFE pilot plant used for validation of marula oil extraction.....	51
Figure 17 Schematic flow diagram of the LECO TFE 2000™ .....	57
Figure 18 A photo (left) and an exploded view of the thimble vessel assembly .....	58
Figure 19 Photo of the porous stainless steel filter (a) 600x magnification .....	58
Figure 20 Exploded view of a schematic for the variable restrictor .....	59
Figure 21 Isometric view of a radial thimble seal model .....	61
Figure 22 The modified LECO TFE 2000 .....	62

## List of tables

Table 1	Calculated influence of time on extraction efficiency as a function of co-solvent.....	17
Table 2	Solubility parameters of Th <sup>+4</sup> in CO <sub>2</sub> .....	21
Table 3	SFE solvent critical parameters (Taylor. 1996) .....	24
Table 4	SFE solvents with displayed molecular geometry .....	26
Table 5	SFE β –diketones.....	29
Table 6:	SFE organophosphates bond structures .....	30
Table 7	MPA of major elements of Steenkampskraal monazite.....	38
Table 8	Average weight % of Th, Ce and Nd in Steenkampskraal monazite .....	39
Table 9	Thorium filter paper extraction procedure conditions .....	43
Table 10	Results for the Kumar experiment .....	44
Table 11	Results of ICP-MS analysis for the thorium standard.....	44
Table 12	SFE Ce <sup>+3</sup> substitution conditions .....	46
Table 13	Ce <sup>+3</sup> α-extraction protocol ThO <sub>2</sub> concentration .....	48
Table 14	Ce <sup>+3</sup> β-extraction protocol ThO <sub>2</sub> concentration.....	49
Table 15	Marula seed oil extraction procedure conditions.....	50
Table 16	Marula seed oil extraction weight .....	51
Table 17	MPA of minor elements of Steenkampskraal monazite.....	63
Table 18	Recalculation of empirical formula from MPA analysis data.....	64

# 1 Introduction

In the nuclear industry radioactive nuclides are used to produce fission reactions. During these reactions large quantities of energy is released, however due to the nature of these reactions it is possible to generate excess neutrons not used in subsequent fission reactions. These neutrons have a probability of being absorbed into nuclear fuel leading to unwanted nuclide formation.

The formation of these nuclides is termed breeding and may pose a significant proliferation risk with the formation of fissile elements such as  $\text{Pu}^{239}$ . Thorium however being only fertile and not fissile, allows for the breeding of  $\text{U}^{233}$  to serve as primary fuel thus avoiding the formation of other potentially dangerous nuclides and increasing proliferation resistance.

Globally the largest source of Th is found in monazite sand, with monazite being a rare earth phosphate mineral most notably found in India, Brazil and in South Africa. The composition of monazite may vary significantly to contain a variety of different lanthanides and actinides including uranium.

The extraction of radioactive nuclides especially U and Pu has been extensively studied leading to solvent extraction processes such as the PUREX process. This process was used for the enrichment of uranium, and plutonium from spent nuclear fuel rods.

Several modifications to this process led to the development of an extraction process for the recovery of thorium from monazite, known as the AMEX process. In addition to conventional solvent extraction techniques, supercritical fluids have been shown to be a successful extraction method for transition metals such as uranium and various other lanthanides from the liquid phase. Furthermore successful extractions of thorium bearing solutions, in this manner, have also been achieved.

More recent work has shown that uranium and thorium is extractable from a cellulose solid matrix (filter paper) using supercritical fluids.

## **1.1 Problem statement**

Current solvent extraction techniques for thorium, such as the AMEX process, hold several disadvantages due to the *in situ* generation of hazardous organic wastes. For thorium to become a preferred nuclear fuel an alternative extraction process to reduce or eliminate the generation of such waste is required, while retaining sufficient extraction efficiency.

## **1.2 Aim**

To review the most prevalent solvent extraction processes for thorium and rare earth elements with specific focus on the feasibility and application of supercritical fluid extraction as a method taking cognisance of crystal chemical requirements and the potential fulfilment thereof for extraction to occur from monazite. To implement the knowledge obtained from the review of solvent extraction techniques in the choice of the supercritical extraction parameters. With the specific focus on the implementation of a supercritical extraction of Th from monazite under the constraints set by the supercritical extraction apparatus.

## 2 Literature Review

The discovery of thorium by Jöns Jacob Berzelius after he erroneously named yttria as thorine was corrected by Berzelius himself in 1828 when he chose to honour Thor, a Scandinavian god with the true discovery of thorium. Thorium is found in many rocks and soils in relative low concentrations, however minerals such as monazite and thorianite may contain more significant concentrations of these elements.

### 2.1 Monazite

Monazite is a natural light rare earth anhydrous phosphate containing a variety of transition elements most notably cerium, lanthanum, neodymium, uranium and small quantities of thorium. Our interest in monazite originates from the thorium content that may be present in the crystal structure. Commercially monazite serves as a source for many rare earth elements and thorium.

Monazite forms part of the space group  $P2_1/n$  (monoclinic) and may preferentially incorporate the larger LREE<sup>1</sup> into a  $REO_9$  polyhedron (Fig. 1), where O (Oxygen) atoms inside the polyhedral coordinates with two REE's<sup>2</sup> and one P (Phosphor) atom. According to Ni *et al.* (1995) monazite can be thought of to consist of polyhedral chains propagating in the [001] direction and sharing tetrahedral edges. This nine fold coordination found in monazite gives rise to nine unique RE-O bond distances resulting in the ability of the crystal to incorporate the LREE's (*op cit*). It is this nine fold coordination exhibited by monazite that gives rise to the question of substitutions in the lattice, while minerals such as xenotime have 8 unique RE-O bond distances and preferentially incorporate the HREE's<sup>3</sup> with coordination of 8 which is a more stable natural arrangement.

---

<sup>1</sup> LREE refers to light rare earth elements.

<sup>2</sup> REE refers to rare earth elements.

<sup>3</sup> HREE's refer to heavy rare earth elements.

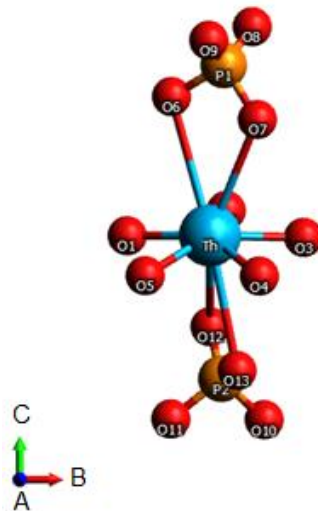


**Figure 1 Structural representation of a monazite polyhedral**

Figure 1 shows the polyhedral  $\text{REO}_9$  chain structure of monazite bonded to two phosphate tetrahedrons with  $[001]$  projected along the C axis. Gaines *et al.* (1997) state that monazite may be thought of as metamict if the crystal contains high amounts of thorium.

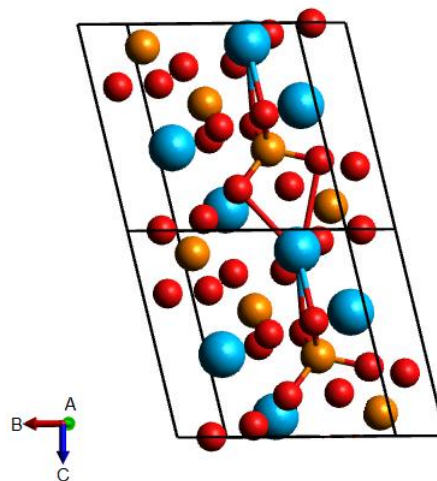


**Figure 2 Representation of a unit cell repetition of monazite**

Figure 2 shows two repetitions of the monazite unit cell containing the polyhedral chain as shown in the previous figure. The colour scheme used for the elements in Figure 1 was copied to the elements shown in Figure 2.

Due to the chemical stability, fusion temperature, optical emissivity and radiological stability of monazite, several possible applications for the mineral were reported by Clavier *et al.* (2011).

*Coating and diffusion barriers.*

The high fusion temperature and chemical resistance to oxidizing environments, allows monazite to be used as a coating material for high temperature applications. One such application studied by Davis *et al.* (1999) uses  $\text{LaPO}_4$  (monazite) sandwiched between two sheets of a woven ceramic fiber for a possible alternative to heat shielding on space vehicles.

*Geochronology.*

The radioactive decay of U and Th leads to the formation of radiogenic Pb (Lead); this radiogenic Pb accumulates inside the monazite lattice and after a period of at least  $100 \text{ Ma}^4$  becomes measurable through electron probe microanalysis. According to Clavier *et al.* (2011) this dating technique is accurate to  $\pm 30\text{-}50 \text{ Ma}$ .

*Luminophors<sup>5</sup> and lasers.*

The use of monazite as a host lattice for doping of various rare earth elements to generate emission spectra with high quantum efficiencies was shown by Song *et al.* (2010) allowing for its use in a wide range of emission devices such as plasma displays.

*Radioactive waste storage.*

Numerous studies have shown the feasibility of a monazite matrix for storage of radioactive nuclides. According to Montel *et al.* (2006) interest in monazite as a spent nuclear storage matrix may be attributed to three factors namely, monazite is commonly found in natural marine environments, therefore showing stability towards leaching processes. Secondly monazite contains varying quantities of uranium and thorium and therefore it should be able to incorporate other transition elements within its crystal structure. Thirdly monazite shows limited metamict behaviour in radioactive environments.

The mining of rare earth minerals such as monazite is carried out all over the world. However economic viability of mining and subsequent extraction of these REE's diminished due to large scale production from China. Xie *et al.* (2014) state that China currently produces 95 % of the world's REE requirements through solvent extraction methods.

---

<sup>4</sup> Ma refers to mega-annum and is equal to  $10^6$  years.

<sup>5</sup> Luminophors refer to an atom or molecule in a host matrix that manifests luminescence.

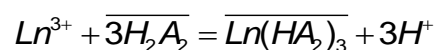
## 2.2 Solvent extraction

From the previous section it is clear that the rare earth minerals such as monazite and rare earth elements contained within these minerals have multiple applications and uses. According to Xie *et al.* (2014) the main commercial sources of rare earth elements are bastnesite (La, Ce)FCO<sub>3</sub>, monazite (Ce, La, Nd, Th)PO<sub>4</sub> and xenotime, YPO<sub>4</sub>.

Solvent extraction can be achieved through three well documented classes namely, cation exchangers (acidic extractions), solvation extractions (neutral extractions) or anion exchangers (basic extractions).

### *Cation exchange*

In acidic extractions two classes of cation exchangers are used namely, carboxylic acids or organic derivatives of phosphorus acids. In China naphthenic<sup>6</sup> acid has been extensively used in the extraction of yttrium primarily from xenotime. The solvent D2EHPA<sup>7</sup> remains one of the most widely used phosphoric acids in the extraction of almost all rare earth elements. The general reaction whereby the cation exchange occurs according to Mason *et al.* (1978) by Xie *et al.* (2014) is written as,



where *Ln* refers to a trivalent rare earth element, *A* to an organic anion and  $3H_2A_2$  is a dimer of the organic acid used during reaction. Over scoring denotes species in organic solution.

<sup>6</sup> Naphthenic acid a carboxylic acid used in solvent extraction.

<sup>7</sup> D2EHPA (Di-(2-ethylhexyl)phosphoric acid)

### Solvation extraction

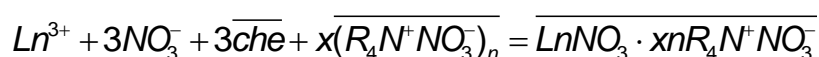
The efficiency of extracting rare earth trivalent elements through the use of chloride and nitrate solutions with the addition of a chelate was shown by Peppard *et al.* (1957) by Xie *et al.* (2014). These extractions were shown to depend on the atomic number of the trivalent atom showing higher efficiency with increase in atomic number. Xie *et al.* (2014) further state that these rare earth neutral nitrate complexes form coordinated bonds with the chelates allowing for extractable complexes and showed the general reaction equation during these types of extraction can be written as,



with  $Ln$  representing the lantanides while  $che$  represents a metal chelate. Xie *et al.* (2014) showed that the extraction of  $Ce^{+3}$  from a sulphate solution employing Cyanex 923 and n-hexane was unaffected by a change in acidity, and the extraction of  $Th^{+4}$  increased with an increase in acidity.

### Anion exchange

In order for metals to be extracted through an anionic complex the presence of a strong anionic ligand is necessary. One such ligand according to Xie *et al.* (2014) may be a quaternary ammonium nitrate salt namely Aliquat 336 (tri-octyl methyl ammonium nitrate) and its reaction may be presented as,



where  $\overline{(R_4N^+NO_3^-)_n}$  denotes the quaternary ammonium nitrate salt. In contrast to solvation and cationic extraction Aliquat 336 in a nitrate medium more readily extracts the LREE's, thus providing a method for removal of the LREE's from process solutions (Xie *et al.* 2014).

The three classes of extraction discussed in this section have been successfully implemented throughout the world in solvent extraction processes. Next six of the most prominent extraction procedures used in rare earth element extraction is presented.

- The Molycorp extraction procedure was used at the Mountain Pass mining facility in California for the primary extraction of europium oxides. This mining and subsequent solvent extraction procedure led to more than 98 % recovery of europium from bastnesite (Xie *et al.* 2014).
- The Rhône-Poulenc extraction procedure according to McGill (1997), by Xie *et al.* (2014) state that the process has the capability to produce 99.9 % of rare earth elements from monazite through solvent extraction. This process initially digests the monazite using NaOH allowing the rare earths to precipitate as hydroxides. Additionally Xie *et al.* (2014) states this process can also produce single rare earth element oxides from bastnesite or euxenite.<sup>8</sup> Furthermore, the Rhône-Poulenc solvent extraction process has been regarded as the standard for industrial producers of rare earth elements.
- Another process namely the AS Megon process is used in the extraction of high purity yttrium from xenotime deposits. This process was first developed by Gaudernack *et al.* (1971) and involves digestion of the xenotime by H<sub>2</sub>SO<sub>4</sub> and filtration by water followed by several scrubbing and stripping stages to produce Y, Tm, Yb and Lu in a single aqueous raffinate solution.
- In South-Africa Mintek extracted rare earth elements from a leachate produced from calcium sulfate sludge in the production of phosphoric acid from apatite. The rare earth elements contained within the apatite were extracted using 40 % (v/v) chelate in Shellsol 2325<sup>9</sup>. This process resulted in a mixture of rare earths with purity of 89-94 %. The rare earth extractant contained significant amounts of middle rare earth elements particularly Nd, Sm, Eu and Ga (Xie *et al.* 2014). Later pilot adaptations were capable of producing different rare earth products from the mixed oxides with the addition of various chelates.
- China remains the world's largest supplier of rare earth elements, of which bastnesite makes up the largest concentration available for processing. The Shanghai Yue Long chemical plant uses a process similar to the Rhône-poulenc process previously discussed. However in the processing of bastnesite the ores are roasted with H<sub>2</sub>SO<sub>4</sub> and the rare earth elements are recovered by solvent extraction using D2EHPA<sup>6</sup>. In an effort to reduce the reagent consumption of D2EHPA, P507<sup>10</sup> has been successfully used to initially extract Th and Ce from the process fluids.

<sup>8</sup> Euxenite is a rare earth mineral composite containing yttrium, tantalum and niobium.

<sup>9</sup> Shellsol 2325 is a mixture of paraffin's cycloparaffin's and aromatics and can be considered a hydrocarbon solvent.

<sup>10</sup> P507 refers to Phosphonic acid (2-ethylhexyl)-mono(2-ethylhexyl) ester

The remaining rare earth elements are removed from a raffinate solution with successive solvent extraction steps.

The PUREX (Plutonium, Uranium, Reduction, Extraction) process remains the only wide scale industrial reprocessing process for Pu and U. Initially the PUREX process was used during the Manhattan project for plutonium extraction and subsequently kept secret for defence purposes. However the PUREX process can be loosely described according to Herbst *et al.* (2011) with the following steps:

- Initially the solids used as nuclear fuel are digested with nitric acid and mixed with a solution of chelates (Typically 30 % vol). This solution serves as feedstock to the separation process.
- Subsequently solvent extraction cycles are used for complete recovery of the desired products. During these steps nitric acid concentration is kept above 0.5M which ensures the plutonium and uranium partition to the organic layer while the fission products stay in the aqueous solution. The recovery and purification of these fuel constituents is achieved through successive liquid-liquid extraction phases, namely scrub and back-extraction cycles.
- Next solidification and vitrification of waste for final treatment and ultimate disposal, with additional steps to waste management that may include evaporation, compositional adjustments and process chemical recovery.
- The final product namely oxides of uranium and plutonium is produced from an aqueous nitrate solution through precipitation and subsequent calcination to the solid metal oxides.

#### Advantages:

- The cycle is continuous therefore a high production rate is achievable.
- High purity of extractant is achievable.
- Minimization of waste through solvent recycling.

#### Disadvantages:

- Degradation of solvents due to hydrolysis and radiolysis.
- Pu can be efficiently extracted but cannot be stripped from DBP<sup>11</sup> and MBP<sup>12</sup>.

---

<sup>11</sup> DBP refers to Di butyl phosphate

<sup>12</sup> MBP refers to Monobutyl phosphate

An alternative to conventional solvent reprocessing known as Super-DIREX is currently being developed by Mitsubishi and Japanese R&D establishments and involves the use of supercritical fluids with chelating agents and is designed to cope with uranium and MOX<sup>13</sup> fuels from light water and fast reactors.

### 2.3 Supercritical fluids

According to Taylor (1996) the first documented observation of the supercritical state was carried out by Baron Cagniard de la Tour in the early 1820's. De la Tour observed that the heating of certain fluids within a closed environment gave rise to the disappearance of the liquid-gas phase boundary.

The term supercritical refers to a condition in which the critical temperature ( $T_c$ ) and critical pressure ( $P_c$ ) of a specific fluid has been reached or exceeded. At and beyond these conditions the fluid can neither be classified as a gas nor a liquid but instead is classified as a supercritical fluid and may have a density approaching that of a liquid and a viscosity similar to that of a gas.

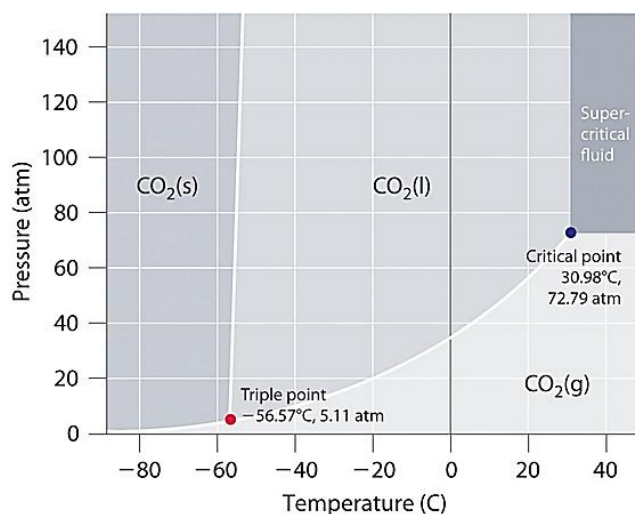


**Figure 3 Phase diagram: CO<sub>2</sub> (after 1)**

Figure 3 above shows the phase dependence of CO<sub>2</sub> including the temperature-pressure regimes of CO<sub>2</sub> in the solid, liquid and gas phases along with the supercritical state. The figure also includes the triple point where CO<sub>2</sub> as a solid, liquid and gas coexists in equilibrium.

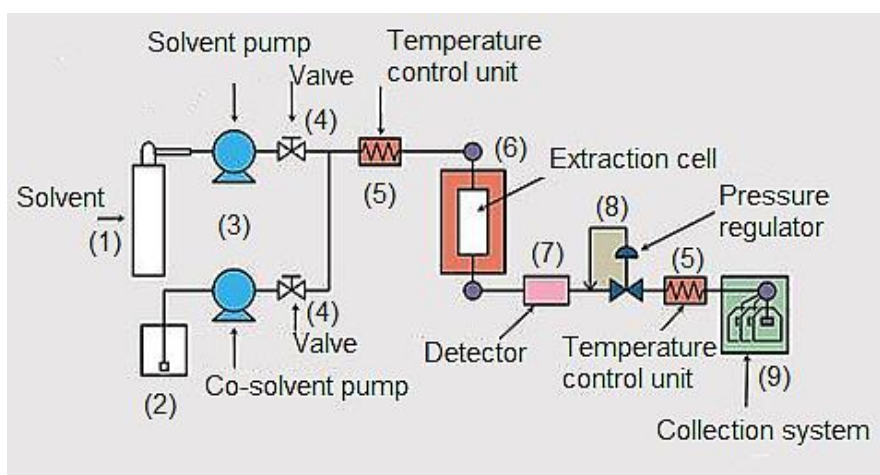
<sup>13</sup> MOX refers to nuclear fuels containing more than one oxide of fissile nuclides.

The critical point as shown in Figure 3 may be defined as, the lowest point where no liquefaction takes place with an increase in pressure and no gas forms with an increase in temperature.

## 2.4 Supercritical Extraction

Supercritical fluid extraction from a solid or a liquid sample has been extensively studied as shown by Herrero *et al.* (2010). This is especially true with respect to commercial applications such as decaffeination of coffee beans. However the use of SFE (Supercritical Fluid Extraction) as part of a rare earth extraction or reprocessing process has yet to find commercial application. As such literature surrounding the direct extraction of transition elements from a mineral phase is limited.

The first study on extracting metals and later transition metals employing supercritical CO<sub>2</sub> was carried out by Laintz & Wai (1992) during which they extracted metal ions (Cu<sup>+2</sup>) from an aqueous solution using modified supercritical CO<sub>2</sub>.



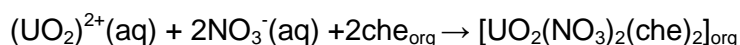
**Figure 4: Schematic of a supercritical extraction setup**

Figure 4 shows a schematic representation of a supercritical extraction setup. The setup consists of (1) a solvent which is the primary fluid used during extraction and is responsible for transfer of the solute from the extraction cell (6) to the collection system (9) through the pressure regulator (8). The extraction cell (6) contains the thimble holders used to hold the samples within the extraction cell. A co-solvent (2) may be added to the system to help facilitate transfer of solute from the host sample to the solvent. Furthermore (3) and (5) represent the pumps and temperature control units used during operations to ensure the desired supercritical condition is achieved. Finally analysis of the solute may be done in an online fashion by various analysis methods such as IR-spectroscopy (7).

### 2.4.1 Liquid phase extraction

In liquid phase extraction the host sample from which the solute is to be extracted is dissolved in an aqueous solution. This solution is then added to the extraction cell. The advantage of this type of extraction is the enhancement of interactions due to increased area of contact between the supercritical fluid and the sample and reduced or no crystal chemical effects due to dissolution of the crystal structure. It is thought that a possible disadvantage to this type of extraction may be large or expensive sample preparation times and excess secondary waste generation.

The extractions of transition metals utilizing dissolution and subsequent supercritical extraction was implemented by Lin *et al.* (1995). The aim of their study was to investigate the removal of uranium and plutonium from acidic nuclear waste generated by dissolving spent nuclear fuel rods. It is claimed (*op cit*) that the reaction during conventional solvent extraction



is probably similar to that of the supercritical reaction taking place. Where *che* may be substituted for other organophosphorus chelates. According to the principle of Le Chatelier an increase in concentration of either nitric acid or nitrate salt in the above equation, drives the reaction to the right hand side. Lin *et al.* (1995) found this principle to hold true for both uranyl and thorium extraction from nitric acid solution.

More recently Ghoreishi *et al.* (2012) showed that the extraction of toxic heavy metals such as uranium, hafnium and zirconium is possible using sulphur containing organophosphorus<sup>14</sup> reagents Cyanex 301 [bis(2,4,4-trimethylpentyl)dithiophosphinic acid] and Cyanex 302 [bis(2,4,4-trimethylpentyl) monothiophosphinic acid]. However to the author's knowledge no indication has been found that the Cyanex chelating agents are more effective than fluorinated  $\beta$ -diketones for thorium extraction.

### 2.4.2 Extraction from a solid phase

In supercritical fluid extraction, solid-phase extraction refers to the solute being contained inside or on the surface of a solid sample with no dissolution of the sample taking place before or during the extraction. Numerous studies have been done on SFE extraction from a solid phase, however nearly all solid phase extraction studies focused on extracting organic material such as oils from seeds. With regard to metal extraction limited studies

<sup>14</sup> Refers to a class of chelating agents discussed in Section 2.6.2

were available for extracting a metal from a solid sample. Shamsipur *et al.* (2001) state that solid phase SFE extraction holds the advantage of reduced consumption and exposure to organic solvent, disposal costs and extraction time. However there may be severe drawbacks to this extraction method if strong bonds are present in the sample as stated by Lin *et al.* (1994).

Lin *et al.* (1993) showed that the extraction of lanthanides and uranyl ions from a solid sample (filter paper) is possible. He (*op cit*) found that the addition of water to the cellulose matrix reduced the interactions of the solute and the matrix facilitating the migration of solute to the solvent. Additionally it was observed the pH range in which supercritical extraction of uranyl ions may occur is much wider than that of conventional solvent extraction by the same organic chelate.

Lin *et al.* (1994) improved on their previous work by introducing an organophosphate chelate TBP (Tributyl phosphate) traditionally used in conventional solvent extraction of metals and the idea of synergistic extraction. During their experimentation a variety of  $\beta$ -diketones were also tested initially using 99.9% pure CO<sub>2</sub> with limited overall efficiency. Subsequently 5% methanol was added to the solvent which showed a marked improvement in the extraction efficiencies obtained. Finally an extraction with TBP was conducted in which they (*op cit*) found the highest overall extraction efficiencies for Th<sup>+4</sup> ions.

Most recently Kumar *et al.* (2009a) extracted thorium and uranium with high efficiency from a tissue paper sample. These extractions were carried out with two organophosphates namely TBP and TOPO<sup>15</sup>. They (*op cit*) found the *in-situ* extraction procedure to be more effective than an online complexation extraction procedure and additionally showed that the extraction of thorium and uranium was possible from a solid sample without the use of acids to dissolve the solid host sample.

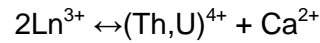
For extraction from solid phase monazite Gaines *et al.* (1997) argued that monazite is one part of a ternary system REEPO<sub>4</sub>-CaThPO<sub>4</sub>-ThSiO<sub>4</sub> in which the Th<sup>+4</sup> ions may be substituted for M<sup>+3</sup> with balanced ionic substitution of silicate (SiO<sub>4</sub><sup>-4</sup>) groups for phosphate (PO<sub>4</sub><sup>-3</sup>) groups.<sup>16</sup>

According to Podor & Cuney (1997) and Terra *et al.* (2008) the substitution of Th<sup>+4</sup> in REEPO<sub>4</sub> may occur by two mechanisms. Firstly as described by Gaines (*op cit*) and secondly by coupled substitution of Th<sup>+4</sup> and Ca<sup>+2</sup> for two REE<sup>+3</sup>. Furthermore Podor &

<sup>15</sup> TOPO is an organic chelate namely tri-octyl phosphine oxide

<sup>16</sup> With M<sup>+3</sup> denoting trivalent metal species.

Cuney (*op cit*) define two parameters whereby the stability of a binary phosphate compound such as  $(A_{0.5}^{+2}B_{0.5}^{+4})PO_4$  may be determined. Furthermore according to Terra (*op cit*) these two parameters gave rise to the general substitution reaction:



The parameters defined by Podor & Cuney (1997) are the mean cationic radii

$$\frac{(r_{A^{+2}} + r_{B^{+4}})}{2}$$

and the ratio of cationic radii in the nine fold coordination state is

$$\frac{r_{A^{+2}}}{r_{B^{+4}}}$$

Podor & Cuney (1997) defines the upper and lower limits for these two parameters under which the crystal structure would be stable and found that:

$$1.10\text{\AA} \leq \frac{(r_{A^{+2}} + r_{B^{+4}})}{2} \leq 1.215\text{\AA}$$

$$1.041\text{\AA} \leq \frac{r_{A^{+2}}}{r_{B^{+4}}} \leq 1.238\text{\AA}$$

These substitution reactions first suggested by Podor & Cuney (1997), Gaines *et al.* (1997) and Terra *et al.* (2008) form the basis of the crystal chemistry approach to the feasibility of this research and the experimental work carried out using monazite as the base mineral for the extraction. The extraction efficiency which is determined or influenced by several intensive parameters is presented next.

## 2.5 Variables affecting SFE

### 2.5.1 Temperature

It is clear from the definition of a supercritical fluid (Section 2.3) that the intensive properties such as temperature and pressure play a significant role in supercritical fluid extraction effectiveness. This was confirmed by Kumar *et al.* (2009b) who clearly showed significant changes in extraction efficiencies depending on several intensive parameters used during extraction. Luque de Castro & Priego-Capote (2010) states that changing the temperature has a triple effect on the overall extraction efficiency namely:

- *Stability of chelates*

The formation of metal-complexes may be temperature sensitive to such an extent that, with a sufficient increase in temperature the chelate used may become unstable and decompose.

- *Extraction kinetics*

Changing the extraction temperature influences the reaction rate of the metal chelate complex formation as well as the substitution rate with which elements may be substituted in the host material as explained in Section 2.4.2.

- *SF density variation*

Changing extraction temperature has an influence on the density of the supercritical fluid. This change in density may affect the extraction kinetics due to the partial molar volumes of the intermediate or final products being greater than the initial constituents potentially having a negative effect on the extraction kinetics.

### 2.5.2 Pressure

Increasing the pressure and thus the density of a fluid results in an increase in viscosity and thus potentially slowing the extraction rate. However there are certain instances where an increase in pressure can enhance the extraction rate. This seeming contradiction may be explained due to the partial molar volume of the products being smaller than the constituents as discussed in the previous section. Furthermore according to Rao *et al.* (2010) Chrastil's empirical relation relates the solubility of a solute to the density in a pure supercritical fluid as follows,

$$\ln S = k \ln \rho + C$$

where  $S$  is the solubility of the solute and  $\rho$  is the density of the supercritical fluid,  $C$  is a temperature dependent variable that consists of thermal properties such as solvating heat, vaporization heat and volatility of the solute and  $k$  is the number of molecules solvating in the solute molecule.

### **2.5.3 Viscosity**

According to Taylor (1996) the viscosity of supercritical fluids can be 50-100 times lower than the viscosity of liquids. Viscosity is dependent on both temperature and pressure and therefore the viscosity of a supercritical fluid approaches that of a liquid with increase in pressure. With regards to temperature an increase results in a reduction in viscosity. The low viscosity exhibited by a supercritical fluid allows for faster diffusion into a solid sample allowing the extraction of solute from the solid samples, otherwise impossible through conventional solvent extraction techniques.

### **2.5.4 Extraction time**

Extraction time may vary widely depending on several variables. According to Luque de Castro & Priego-Capote (2010) the effects to be taken into consideration during extraction include solvent power, variability of host sample structure and reaction kinetics. If a continuous flow extraction is chosen another variable is introduced namely the equilibration time. This may be thought of as the time required for interaction between the solute and the solvent under SFE extraction conditions. The extraction efficiency is highly dependent on extraction time as shown in Table 1 were extraction efficiency of aromatic compounds varies between less than 1 % to above 80 %. Furthermore from Table 1 it is clear that the selection of a co-solvent plays a significant role in the extraction efficiency, and is further discussed in Section 2.6.3.

**Table 1 Calculated influence of time on extraction efficiency as a function of co-solvent**

SFE extraction efficiency with variations in co-solvent concentration and extraction time of an aromatic compound from XAD-4<sup>17</sup> resin (Luque de Castro & Priego-Capote. 2010).

Extraction time (min)	CO <sub>2</sub>	Co-solvent				
		6%	6%	6%	6%	12%
		methane	acetone	EtOAc <sup>18</sup>	hexane	hexane
15	-	0.9	-	5.5	12.5	11.9
30	0.1	1.5	-	15.1	37.3	37.3
60	0.4	59.6	25.1	36	78.6	74.5
90	8.7	78.6	74.2	76.4	81.5	76.4
120	49.6	84.5	70.6	55.7	92.1	74.7
180	83.9	84.6	70.2	78.4	73.2	56.1

### 2.5.5 Phase behaviour

As with extraction time the phase behaviour of supercritical fluids and complexes thereof may severely influence the extraction efficiency. Previously the definition of a supercritical fluid (Section 2.3) included both a pure fluid and a mixture of several fluids. However these mixtures may exhibit critical parameters that are different compared to the pure state of each component. Thus Figure 3 represents only the phase diagram and critical point of a pure CO<sub>2</sub> fluid. According to Darr & Poliakoff (1999) a chemical reaction involves at least three components such as products, solvent and starting materials. However in most cases more complex reactions may occur during SFE. They (*op cit*) state as an example the system CO<sub>2</sub>/H<sub>2</sub> where there is a narrow temperature range in which a single phase mixture may separate into two compounds with an increase in pressure due to the existence of a miscibility gap.

<sup>17</sup> XAD-4 resin refers to non-ionic macroreticular resin that adsorbs and releases ionic species through hydrophobic and polar interactions.

<sup>18</sup> EtOAc refers to Ethyl Acetate

Due to this type of possible phase behaviour a pitfall in both solid and liquid extraction is the formation of a third compound due to solubility limitations of the solvent-solute complex, resulting in reduced extraction efficiencies.

### **2.5.6 Grain size**

Grain size plays an important role in supercritical extractions. With sufficient solvating power the extraction rate may be increased by increasing surface area or porosity of the sample. One method of increasing the surface area is through grinding. Some samples may swell or exfoliate with the addition of supercritical solvents allowing ease of access to the desired solute. This phenomenon is predominant in polymers and organic materials. However if the matrix is fully permeable by the supercritical solvent, grain size has no influence extraction efficiency but only the extraction rate.

### **2.5.7 Crystal chemical parameter**

The crystal chemical parameter may be loosely defined as the effect the crystal structure has on the solute to inhibit its removal from the atomic structure and varies significantly with the way in which the solute interacts with this structure.

The interaction between the sample and the solute may involve adsorption or absorption. Furthermore the type of sample from which the solute is to be extracted is also of importance as it may be within a rigid or expandable, porous or non-porous material. The influence the crystal chemical effect has on extractions was clearly shown by Lin *et al.* (1994) in which addition of water to the extraction of thorium from a filter paper increased the extraction efficiency due to the water competing for the active sites in the host sample.

### 2.5.8 Solubility

According to Taylor (1996) the ability to remove a solute from a material may depend in varying degrees on several factors. These include:

- Solubility of the solute in the SF (supercritical fluid).
- Analyte-sample interactions.
- Analyte location within the sample.
- Porosity of the sample.

Dean (1993) describes the interaction between components of a supercritical fluid extraction system as follows:

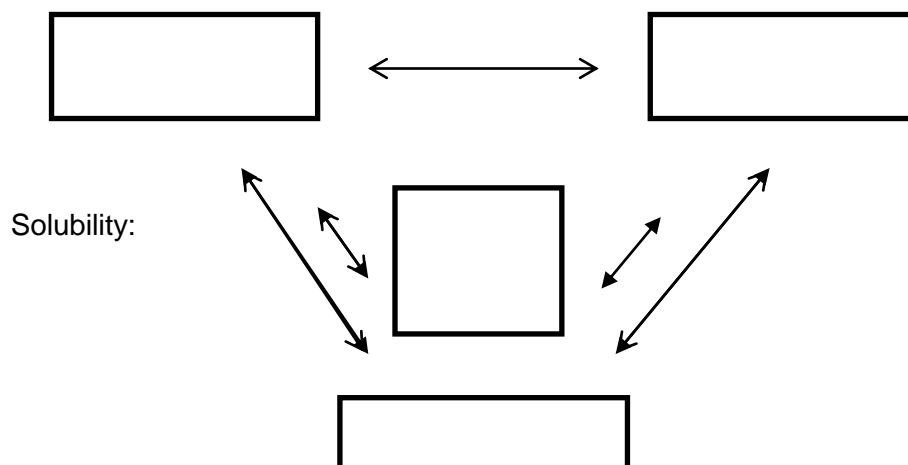


**Figure 5 Representation of interaction between SFE components (after Dean. 1993)**

Figure 5 shows the interrelation between the three components of a SFE extraction. Furthermore the figure lists the effects the supercritical fluid may have on the sample structure and the variables affecting solute-solvent solubility.

Solubility in this study is a measure of how much  $\text{Th}^{+4}$  can be dissolved into the supercritical solvent before saturation occurs. Solubility therefore influences the rate at which the extraction can occur. Solubility is influenced by two factors namely:

- The stability of the solute, modifier and chelates.
- The solvating strength of the supercritical fluid which in turn is a function of the fluid density.

Effective prediction of solubility for the solute helps reduce development time. Furthermore the overall feasibility of the extraction may also be determined.

One approach to determine solubility is solubility parameter theory. This theory described by King & Friedrich (1990) and presented by Dean (1993) relies on four parameters namely, miscibility pressure, maximum solubility pressure, fractionation pressure range and the physical properties of the solute.

- *Miscibility pressure*

The miscibility pressure refers to the pressure at which the solute becomes miscible in the supercritical fluid, therefore at the miscibility pressure a two component system consisting of a supercritical fluid and a solvent becomes a single compound. The miscibility pressure may vary with relation to the solute concentration in the supercritical fluid. Furthermore the miscibility pressure may be used as an initial starting point for extraction pressure.

- *Maximum solubility pressure*

This variable refers to the pressure at which maximum solubility of the solute in the supercritical fluid is achieved and typically occurs when the solubility parameter of the fluid equals the solubility of the solute.

- *Fractionation pressure range*

This parameter is the range in which the solute miscibility varies from zero at the miscibility pressure to a maximum at the “maximum solubility pressure”. Due to the variation of miscibility with variations in pressure this effect may lead to selection of different solutes at different pressures having a selective enriching effect of a single solute.

- *Physical properties of the solute and solubility in supercritical solvent*

The physical state and melting point of a solid is of importance when determining the solvent-solute solubility, primarily due to the enhanced solubility of liquids in the supercritical state. One method of correlation was proposed by King & Friedrich (1990) who introduced the variable, reduced solubility  $\delta$  which is defined as,

$$\delta = \frac{\delta_1}{\delta_2}$$

with  $\delta_1$  being the solubility variable of the solvent and  $\delta_2$  the solubility variable of the solute. The solubility variables are then calculated using,

$$\delta_1 = 1.25 \sqrt{P_c} \cdot \left( \frac{\rho}{\rho_{liq}} \right)$$

with  $P_c$  the critical pressure of the solvent,  $\rho$  the density of the supercritical fluid and  $\rho_{liq}$  the density of the fluid in the liquid state.

Whereas  $\delta_2$  may be calculated as,

$$\delta_2 = \sqrt{\left( \frac{\Delta \varepsilon}{\Delta v} \right)}$$

with  $(\varepsilon)$  is the energy of vaporization at a given temperature and  $(v)$  the molar volume of the solute. The values represented in table 2 for both CO<sub>2</sub> and Th<sup>+4</sup> were obtained from standard reference sources.

**Table 2 Solubility parameters of Th<sup>+4</sup> in CO<sub>2</sub>**

CO <sub>2</sub>	
Critical density (kg/m <sup>3</sup> )	467.6
Liquid density (kg/m <sup>3</sup> )	593.31
Critical pressure (kPa)	7377
$\delta_1$	84.614
Th <sup>+4</sup>	
Energy of Vaporization (kJ/mol)	530
Molar volume (m <sup>3</sup> /mol)	1.98E-05
$\delta_2$	5173.749
Reduced solubility parameter	
Th <sup>+4</sup> in pure CO <sub>2</sub>	0.0163

Equating these values yields a low reduced solubility parameter for  $\text{Th}^{+4}$  in pure  $\text{CO}_2$  as shown in Table 2. This is expected as Kumar *et al.* (2009b) showed thorium has limited solubility in pure  $\text{CO}_2$ .

Thus the addition of chelates reviewed in the next section is necessary to increase solubility of the solute in the solvent.

## 2.6 Solvent, chelates and modifiers

### 2.6.1 Solvent

The use of a specific solvent for the extraction of a metal is chosen on the basis of several considerations. These included the choice of critical parameters  $T_c$  and  $P_c$ , low volatility, good solubility, relatively low toxicity and abundance of previous studies with regards to metal extraction and more specifically of lanthanide and actinide SFE extractions.

This selection is made on a semi empirical basis by defining a scale on which the solvating power of each relevant solvent can be listed and compared.

A scale to correlate different solvent interactions (known as the  $\pi$ -scale) was developed by Kamlet *et al.* (1983). This scale is an index for solvent dipolarity/polarizability which can be interpreted as the ability of the solvent to stabilize a charge by way of its dielectric effect.

The dielectric effect according to Luque de Castro & Priego-Capote (2010) is the most relevant physico-chemical property for defining the solubility of fluids in general. The dielectric constant of water is a good example of how solvating power changes with variation of pressure/density and temperature. The dielectric constant of water at ambient conditions is approximately 78.5 resulting in effective masking of ionic charges. With increase in temperature and decrease in pressure they (*op cit*) state that the dielectric constant at 1000 °C is approximately 12 and under these conditions supercritical water may act as a non-polar solvent.

Variation of the dissolving power as a function of the reduced density for various supercritical fluids

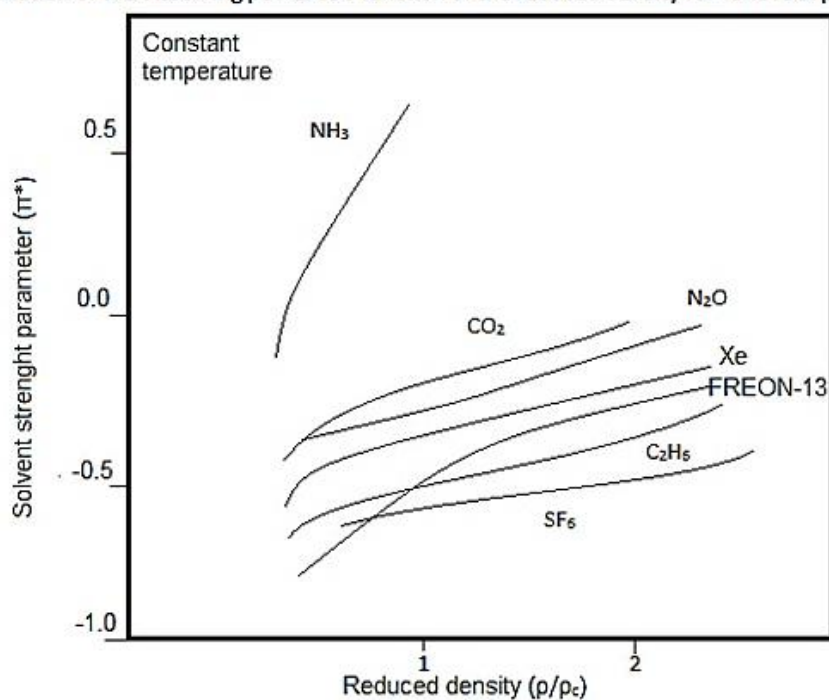
**Figure 6 Parameter  $\pi^*$  for solvability (Luque de Castro *et al.* 2010)**

Figure 6 shows the solvent strength for several well-known SFE solvents. From this figure it is seen that  $\text{NH}_3$  according to the  $\pi$  scale is the most favourable solvent followed by  $\text{CO}_2$  and various other solvents.

Table 3 contains the critical parameters of several known supercritical fluids and a subsequent discussion on each fluid concluding in the final choice of a solvent.

**Table 3 SFE solvent critical parameters (Taylor. 1996)**

Solvent	Critical Temperature (°C)	Critical Pressure (bar)
NH <sub>3</sub>	132.4	113.5
CO <sub>2</sub>	31.1	73.8
N <sub>2</sub> O	36.6	72.4
Xe	16.7	58.4
C <sub>2</sub> H <sub>6</sub>	32.4	48.8
CH <sub>3</sub> OH	240.1	80.9

- *NH<sub>3</sub> (Ammonia)*

Ammonia has a dipole moment of 1.42D with molecular geometry shown in Table 4. Ammonia is used preferably with polar substances however the relatively high critical parameters, corrosivity and toxicity of ammonia is inhibitive for general use without specialized equipment.

- *CO<sub>2</sub> (Carbon Dioxide)*

Carbon dioxide is a non-polar molecule (Table 4) with relatively moderate critical parameters, benign to the environment and non-toxic. Owing to these favorable parameters CO<sub>2</sub> has been used in large scale industrial applications. However due to the lack of polarity CO<sub>2</sub> performs poorly as solvent for polar extraction.

- *N<sub>2</sub>O (Di-nitrogen oxide)*

Di-nitrogen oxide has a small permanent dipole as seen by the geometry displayed in Table 4. There are notable differences in extraction efficiencies with N<sub>2</sub>O and CO<sub>2</sub> as solvents. More specifically solutes from adsorbed matrices show N<sub>2</sub>O as being more efficient than CO<sub>2</sub> (Taylor 1996).

- *Xe (Xenon)*

Although the critical parameters for xenon are some of the lowest for all investigated solvents, no studies have been found which employ xenon as supercritical solvent for metal extraction. Finally due to relative scarcity and a lack of proper laboratory instrument support for Xe this solvent has yet to be fully realized in metal SFE extractions.

However the use of xenon as solvent holds particular advantages for on line analysis methods such as IR<sup>19</sup> spectroscopy of SFE extractants. According to Darr & Poliakoff (1999) xenon is completely transparent throughout the mid and far IR spectrum at room temperature which may otherwise influence analysis results.

- *C<sub>2</sub>H<sub>6</sub> (Ethane)*

Ethane is a non-polar molecule as seen in Table 4 with relatively low critical parameters (Table 3); however the use of ethane as solvent is limited due to its high volatility. From Figure 6 the solvability parameter ( $\pi^*$ ) for ethane is less than that of the other solvents.

- *CH<sub>3</sub>OH (Methanol)*

The use of methanol as solvent is generally prohibitive due to its high critical temperature, however methanol exhibits high solvent strength and is subsequently used as co-solvent (also in this study).

---

<sup>19</sup> IR: Infra-Red

The final consideration in choice of solvent according to Taylor (1996) should be the available purity of the solvent. He (*op cit*) reported cases in which the detection limit was determined by the impurities in the CO<sub>2</sub> solvent and not the detector.

**Table 4 SFE solvents with displayed molecular geometry**

Ammonia(NH <sub>3</sub> )	$\begin{array}{c} \text{H} \\   \\ \text{N}-\text{H} \\ / \\ \text{H} \end{array}$
Carbon Dioxide(CO <sub>2</sub> )	$\text{O}=\text{C}=\text{O}$
Di-nitrogen oxide(N <sub>2</sub> O)	$\begin{array}{c} \text{O}-\text{N} \\ / \\ \text{N} \end{array}$
Ethane(C <sub>2</sub> H <sub>6</sub> )	$\begin{array}{c} \text{H} \quad \text{H} \\   \quad   \\ \text{H}-\text{C}-\text{C}-\text{H} \\   \quad   \\ \text{H} \quad \text{H} \end{array}$
Methanol(CH <sub>3</sub> OH)	$\begin{array}{c} \text{H} \\   \\ \text{HO}-\text{C}-\text{H} \\   \\ \text{H} \end{array}$

### 2.6.2 Chelate

Due to the lack of polarity in solvents such as CO<sub>2</sub> and the resulting weak solute solvent interaction, direct extraction of metals from both liquid and solid states has been proven to be ineffective as cited by various literature sources.

The International Union of Pure and Applied Chemistry (IUPAC) defines a chelate as a ligand that forms, or is in the presence of two or more separate coordinated bonds with a central metal atom. Thus a chelate is considered a ligand once a bond with a metal has been formed.

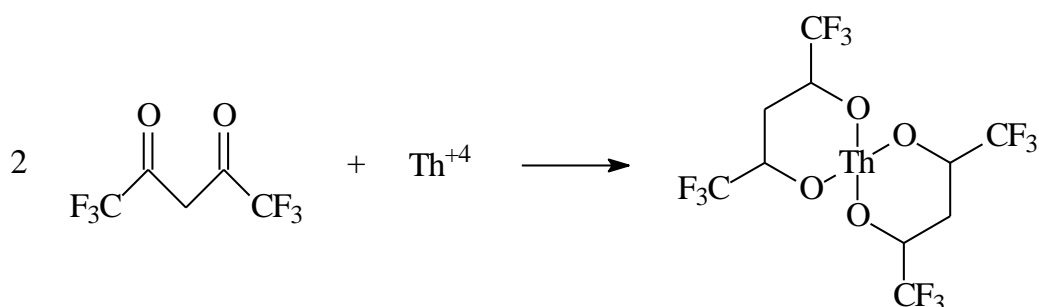


**Figure 7 Structure illustration of a chelating reaction**

Figure 7 shows an illustration of a typical  $\beta$ -diketone chelate (HFA<sup>20</sup>) and its reaction with Th<sup>4+</sup> to form a metal ligand.

The selection of an adequate chelating agent is therefore of crucial importance to ensure good solubility of the ligand in the supercritical fluid. Early work by Wai & Wang (1997) present several classes of chelating agents of importance to SFE:

#### *Dithiocarbamates*

These chelates are derivatives of dithiocarbamic acid and are effective for pre-concentration of trace elements from solvent extraction. The study to show metal extractability by SFE using a dithiocarbamate was carried out by Laintz & Wai (1992) in which Cu<sup>+2</sup> ions were extracted from an aqueous solution made by dissolving solid Cu(NO<sub>3</sub>)<sub>2</sub> in deionized water. The extraction was carried out in the presence of LiFDDC (Lithium bis (trifluoroethyl) dithiocarbamate) as the chelate.

Applications of dithiocarbamate are limited due to the instability which the chelate experiences in the presence of water. This inherent instability according to

<sup>20</sup> HFA is a fluorinated  $\beta$ -diketone with the IUPAC name hexafluoroacetyl-acetone.

Wai & Wang (1997) leads to the need for excess amounts of dithiocarbamate in extractions to achieve good SFE efficiencies.

Finally they (*op cit*) state that pressure has a significant influence on the solubility of dithiocarbamate reagents in some cases improving the solubility of the chelate in the solvent. Figure 8 below shows the bond structure of the chelate LiFDDC which is a typical dithiocarbamate.

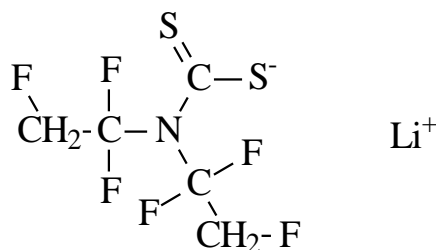


**Figure 8 Bond structure illustration of Li(FDDC)**

### *β-diketones*

The class of chelates known as  $\beta$ -diketones is widely used in metal extractions.  $\beta$ -diketones are all liquids at ambient conditions and form neutral metal complexes through enolate anions (reaction below). The addition of fluorine to the  $\beta$ -diketones increases the effectiveness of the chelate to form metal bonds. This according to Wai & Wang (1997) is due to the electron withdrawing effect the fluorine substitution has, thereby increasing the ligand acidity. However it should be noted that the presence of moisture on chelates such as on HFA<sup>18</sup> causes an irreversible hydrolysis<sup>21</sup> reaction. It is unknown if this decomposition occurs with all  $\beta$ -diketones.

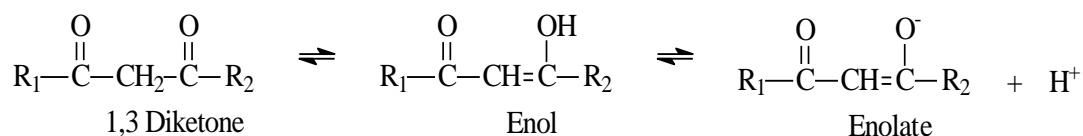


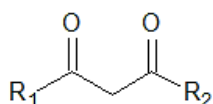
**Figure 9 Bond structure illustration of enolate formation during metal complexation**

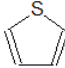
<sup>21</sup> Hydrolysis refers to the cleavage of chemical bonds through the addition of water

Figure 9 shows a simplified illustration of the reaction a  $\beta$ -diketone undergoes to form an enolate anion. It is thought this reaction occurs to produce the overall ligand formation as shown in Figure 7.

Table 5 shows some of the most commonly used  $\beta$ -diketones for SFE processes.

**Table 5 SFE  $\beta$ -diketones**



$\beta$ -diketone	Abbreviation	R <sub>1</sub>	R <sub>2</sub>	Mol. Wt.	B.P (°C)
Acetylacetone	AA	CH <sub>3</sub>	CH <sub>3</sub>	100.12	139
Trifluoroacetylacetone	TFA	CH <sub>3</sub>	CF <sub>3</sub>	154.09	107
Hexafluoroacetylacetone	HFA	CF <sub>3</sub>	CF <sub>3</sub>	208.06	71
Thenoyltrifluoroacetone	TTA		CF <sub>3</sub>	222.18	104
Heptafluorobutanoylpivaroyl methane	FOD	C(CH <sub>3</sub> ) <sub>3</sub>	C <sub>3</sub> H <sub>7</sub>	296.18	33

#### *Organophosphorus reagents*

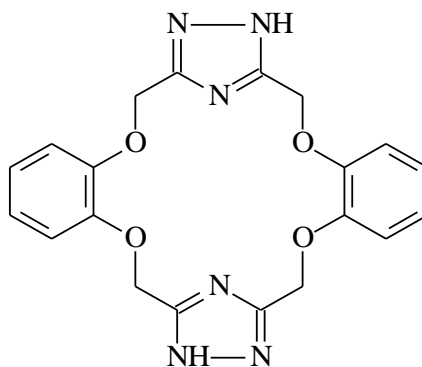
The use of organophosphorus chelates started with conventional extractions of actinides and was quickly adapted to supercritical fluid extraction of metals. TBP (tri butyl phosphate) as shown in Table 6 is one such organophosphate and is used extensively in the extraction and separation of U and Pu via the PUREX process as described in Section 2.2. According to Wai & Wang (1997) these organophosphorus chelates form coordinated salts with the lanthanides and actinides through the P=O group. Herbst *et al.* (2011) showed that the affinity of TBP for trivalent and lower cations is almost zero while the affinity for tetravalent and higher oxidation states cations is high demonstrating the possibility for selective extraction. The study by Wai *et al.* (*op cit*) also showed that the phosphorous containing chelate Cyanex 302 appear stable in supercritical CO<sub>2</sub>. Table 6 shows various organophosphate chelates used in supercritical fluid extractions.

**Table 6: SFE organophosphates bond structures**

List of Organophosphates	
Name:	Structure:
TBP (Tributyl phosphate)	
TOPO (Tri-octylphosphine oxide)	
Cyanex 301 (Bis 2,4,4-trimethylpentyl-dithiophosphinic acid)	
Cyanex 302 (Bis (2,4,4-trimethylpentyl)-monothiophosphinic acid)	
D2EHPA Di(2-ethylhexyl) phosphoric acid	

*Macro cyclic ligands*

Macro cyclic polyether or crown ethers can form charged or neutral metal chelates and may selectively bond different sized cations according to the cationic radius of the metal species to form selective complexes in processes such as SFE.

**Figure 10 Bond structure illustration of crown ether**

### *Other ligands*

From the literature review it is clear that in metal extractions fluorinated chelates perform better as ligands than non-fluorinated counterparts however, according to Wai & Wang (1997) the costs involved with fluorination is prohibitive to the use in SFE. One possible alternative may be hydrocarbon based aliphatic substitutions. These chelates show solubilities approaching that of fluorinated chelates and may have large scale application. To the author's knowledge this type of ligand has yet to be used in a SFE process of transition metals.

### **2.6.3 Choosing a modifier**

Previously the ineffectiveness of pure CO<sub>2</sub> as a metal extraction solvent was stated and the need defined for a modifier agent to be added to the solvent in order to modify the solvent polarity. This is known as the Entrainer Effect which may be defined as an increase in solubility of the solute in the solvent with the addition of a small amount of secondary solvent. These modifiers may interact with either the solvent or metal atoms in one of two ways namely, they may coordinate with a central metal atom to reduce the overall polarity of the metal species, or the modifier may interact with the solvent to increase its polarity. Shamsipur *et al.* (2001) calculated the solubility of uranyl nitrate in methanol at different conditions and showed methanol to have a good solubility for transition elements.

Various different modifiers are available however only two namely methanol and ethanol were considered for this research due to limitations of the extraction apparatus.

### **2.6.4 Synergistic extraction**

In order to potentially remove the modifier and therefore large amounts of secondary waste a synergistic extraction process may be followed. The synergistic extraction procedure avoids using a co-solvent such as methanol and instead uses a secondary chelate. Work done by Lin & Wai (1994) showed that the extraction of lanthanides with limited or no modifier present is possible. They (*op cit*) furthermore stated that the efficiency of a synergistic extraction depends on the structure of the fluorinated  $\beta$ -diketones used. Darr & Poliakoff (1999) found that a strong synergistic effect takes place with the use of HFA a fluorinated  $\beta$ -diketone and TBP an organophosphate. However more recent literature (Kumar *et al.* 2009) have shown the continued use of modifiers in extraction of radio-active elements may be due to the hydrolysis and radiolysis experienced by chelates used in the extraction of radioactive contaminated species such as in reprocessing of nuclear fuel.

## 2.7 Trapping

The efficient trapping of solutes in a collection vessel is one of the most important parts of the extraction process. This is due to the importance of overall extraction efficiency depending heavily on the trapping effectiveness. Taylor (1996) state that extractions may be viewed as a three step process, initial transfer of the solute from the host sample to the supercritical state thereafter the transfer from the extraction vessel to a collection system and finally efficient collection of the solute in the collection vessel.

Furthermore it may not be possible to quantify the extraction efficiency if the trapping effectiveness is inadequate. Some of the trapping methods used in SFE are discussed below.

### *Liquid trapping*

Liquid trapping is the most used form of trapping due to simplicity and ease of operation. However for the trapping efficiency to be sufficient the solute must show high miscibility in the trapping solution and the solvent must be compatible with post extraction analytical techniques.

During this trapping method the flow through the restrictor should generally be kept below 1 mL/min as larger volume flow rate of gasses may result in violent bubbling leading to loss of trapping solvent and inefficient trapping. Depending on the volatility of the trapping solvent the addition of more solvent during extraction may be required to maintain an immersed state in the collection vial. Taylor (1996) state that If the restrictor outlet is not immersed in solvent trapping may depend on the transfer efficiency of the solute from the gas phase to the collection solvent.

The trapping efficiency may also significantly vary with cooling or heating of the solvent in the collection vessel. Generally cooling the collection vessel yields more optimum results (Taylor 1996).

### *Inert solid trapping*

This method of trapping relies completely on the precipitation of the solute in the collection vial. In order to better facilitate the precipitation of solute the collection vial may be cooled to further immobilise the solute. This method of trapping works best for non-volatile solutes in pure solvent extractions. According to Taylor (1996) this method of trapping is not advised for analytical extractions as low concentrations of solute may not be sufficiently trapped.

### *Active sorbent trapping*

With active solid sorbent trapping a chromatographic stationary sorbent material is utilized. The particles of the solid sorbent should exceed the aperture size of frits<sup>22</sup> or screens in the trap housing to prevent accidental loss of trap materials. Trapping with this method may occur in two mechanisms namely cryogenic trapping and partitioning. Due to the multiple trapping mechanisms involved with active solid traps, CO<sub>2</sub> flow rates may be increased beyond the general rule for liquid trapping. A further advantage of active solid trapping over inert solid traps may be greater selectivity in extraction of a specific solute, due to an appropriate choice of trapping sorbent.

## **2.8 Extraction protocol**

For SFE processes two protocols exist by which the system may be pressurised, maintained and depressurized during extractions.

- *Static flow*

Static flow extraction refers to the system being pressurized to a set pressure and temperature where after no additional solvent is added to the extraction vessel, thereby fixing the amount of solvent that may interact with the sample atomic structure and solute bonded in this structure. Static mode extraction has the advantage of preserving supercritical fluid and modifiers. This mode of extraction may suffer from insufficient fluids being used not allowing for complete extraction of solute from the host sample. A static flow extraction is followed by a continuous flow protocol to depressurize the system.

- *Continuous flow*

With a continuous flow protocol the final pressure and temperature is reached while a continuous flow of solvent, co-solvent and chelate is supplied to the sample. A possible concern with this mode of extraction is contamination due to impurities found in the solvent. Furthermore continuous flow extraction has a higher probability of co-extraction of secondary and possibly unwanted solutes from the sample as well as the possibility of the host sample being flushed from the reaction vessel to the collection vial. Despite these drawbacks to continuous flow extraction this protocol of extraction provides faster extraction times. Furthermore continuous protocols are more applicable to online analysis methods. According to Taylor (1996) this protocol of extraction is used in over 90 % of reported applications for SFE processes.

---

<sup>22</sup> The frit (Figure 19) consists of a porous stainless steel disc to prevent flushing of materials from the extraction vessel.

## 2.9 Summary

Monazite was investigated through a literature study to determine the feasibility of removing REE's from the crystal structure. The co-ordination chemistry of the crystal structure was shown to be an unfavourable arrangement when compared to other arrangements such as that of xenotime giving rise to the question of extractability.

Subsequently the literature study focused on a review of known solvent extraction techniques for monazite and various other REE containing minerals. From this review the literature revealed the feasibility of supercritical fluid extraction of metals and transition metals (Section 2.4).

However these extractions were shown to be inefficient if co-solvents and chelates were not used due to the lack of polarity exhibited by solvents such as CO<sub>2</sub>. A study from literature however, revealed a suitable solvent, co-solvent and chelate comparing several different compounds in each case.

Subsequently the literature revealed various parameters of importance for SFE extractions as covered in Section 2.5. The section concluded with a discussion on relevant trapping methods believed to greatly influence the overall extraction efficiency and the possible protocols for SFE.

## 3 Experimental work

### 3.1 Mineralogical characterization

#### *Material acquisition*

Monazite ( $\approx 2$  kg) was procured from the Steenkampskraal mine in South-Africa. The grains in the sample were roughly  $200 \mu\text{m}$  in size. The size of the grains was visually confirmed through scanning electron microscope inspection. Investigation regarding the grain size was done via sieving of the original sample.

#### *Sample preparation*

About 2 g of monazite grains was covered and encapsulated in clear epoxy resin and after subsequent setting of the resin this composite was polished until a flat surface was obtained exposing the monazite grains. Figure 11 shows the prepared monazite sample. This sample of embedded monazite grains was then subjected to a scanning electron microscope (SEM) with attached energy dispersive spectroscopy (EDS) for analysis.



**Figure 11** Photo of a polished sample of monazite grains imbedded in an epoxy resin.

Another sample of monazite from the Steenkampskraal mine batch material was encapsulated in a clear resin on a thin glass plate and subsequently polished to an acceptable thickness ( $30 \mu\text{m}$ ) for Electron Microprobe elemental point analysis through wavelength dispersive spectroscopy (WDS).

*Th, Ce and Nd element distribution*

The distribution of Th, Ce and Nd in the sample was determined on a qualitative basis using a SEM in an area scan mode. With the scanning time set to 100 s and a capture time of 0.1 s in the BSE<sup>23</sup> mode.

Figure 12 represents the elemental distribution obtained through SEM EDS analysis for phosphorus (red) and cerium (green) of the same area as the BSE image (grey scale). The neodymium (blue), thorium (purple) and calcium (orange) elemental distribution obtained in this manner is also shown for the monazite grains.

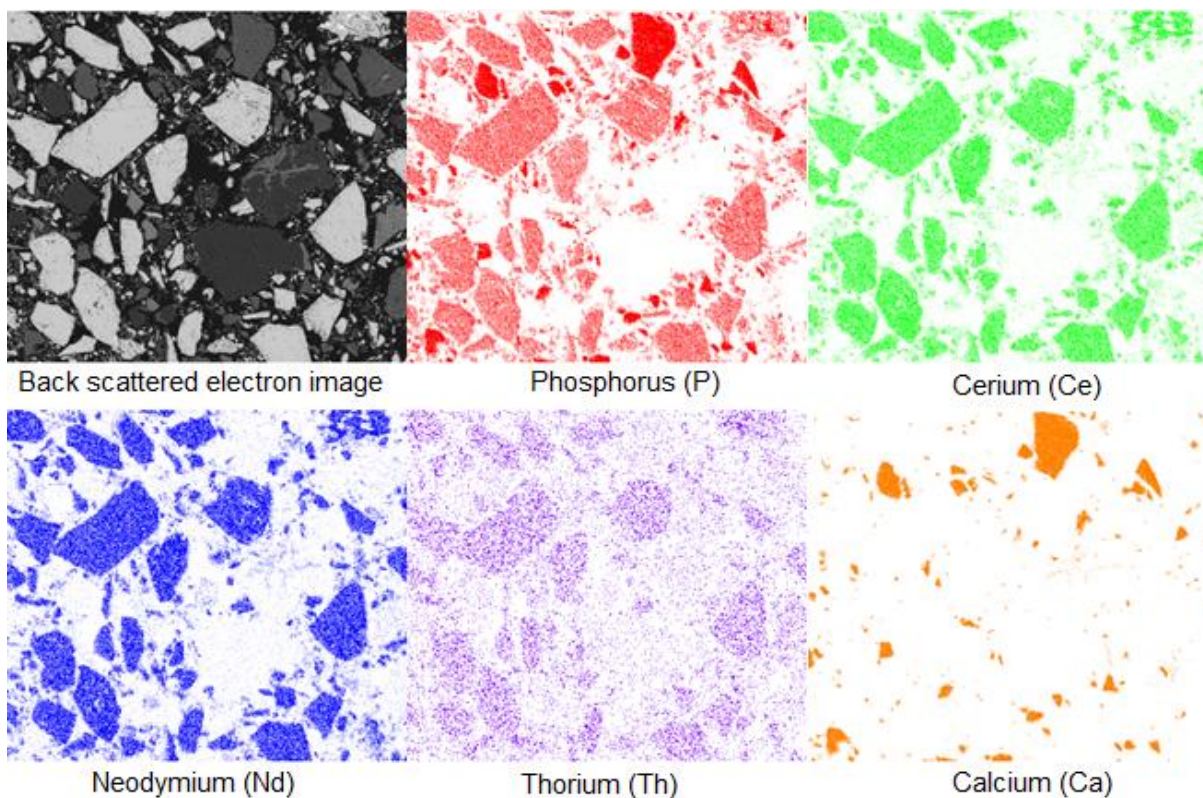


**Figure 12 BSE image of monazite grains with element distribution maps**

<sup>23</sup> BSE refers to back scattered electrons

*Th, Ce and Nd concentration*

Fifteen unique detection positions on four grains (Figure 13) were chosen for electron microprobe analysis (MPA) on the polished grain slide. The analyses were carried out with a Cameca electron microprobe in wavelength dispersive mode (WDS) at the analytical facility of the University of Johannesburg, employing an electron beam with standardisation of oxides for the elements of interest.

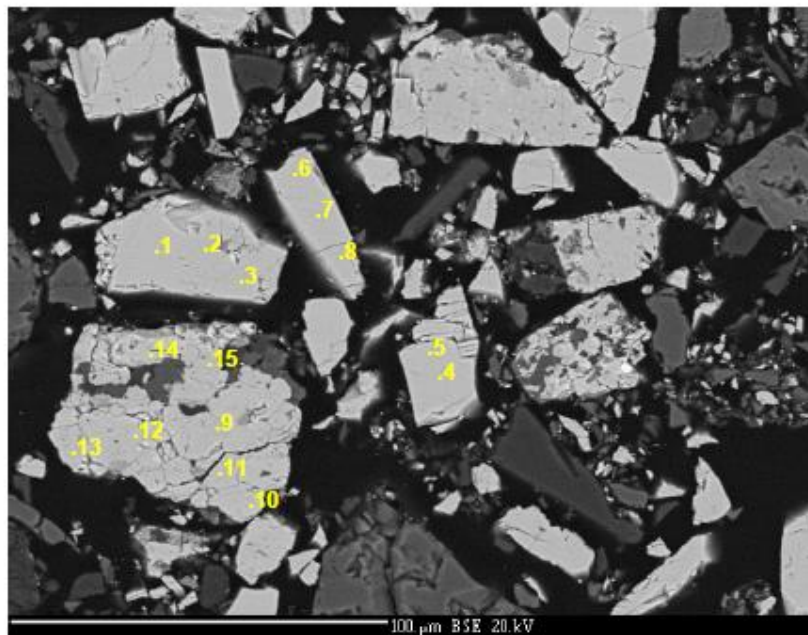


**Figure 13 Microprobe BSE image of monazite grains illustrating 15 analysed points.**

Table 7 shows the concentration of each investigated element as a weight % of the corresponding oxide. The 15 analyses points in Fig 13 are indicated in the ID column of Table 7.

**Table 7 MPA of major elements of Steenkampskraal monazite  
(weight % as elemental oxide)<sup>24</sup>**

ID	CaO	Ce <sub>2</sub> O <sub>3</sub>	La <sub>2</sub> O <sub>3</sub>	Nd <sub>2</sub> O <sub>3</sub>	O	PO <sub>4</sub>	SiO <sub>2</sub>	ThO <sub>2</sub>	Y <sub>2</sub> O <sub>3</sub>
1	0.83	22.94	10.68	9.65	27.16	12.78	0.47	7.62	1.81
2	0.85	22.92	10.61	9.43	27.02	12.74	0.41	7.78	1.79
3	0.83	23.00	10.72	9.54	27.20	12.81	0.45	7.82	1.76
4	0.85	22.77	10.58	9.61	26.93	12.67	0.43	7.72	1.76
5	0.86	23.09	10.61	9.58	27.18	12.76	0.47	7.71	1.81
6	0.73	23.91	11.27	9.62	27.34	13.00	0.37	6.47	1.66
7	0.70	23.9	11.18	9.60	27.19	12.90	0.40	6.34	1.67
8	0.75	23.75	11.16	9.41	27.33	13.04	0.41	6.72	1.53
9	0.38	25.14	11.98	10.33	27.02	12.73	0.46	5.20	0.61
10	0.46	24.44	10.79	9.44	26.07	12.28	0.53	6.45	0.51
11	0.40	24.37	11.77	10.11	26.02	12.09	0.49	5.60	0.62
12	0.51	23.69	11.88	9.88	26.30	12.08	0.51	6.90	0.45
13	0.32	26.5	11.46	9.51	27.19	12.68	0.62	6.56	0.62
14	0.51	25.41	11.84	10.03	27.49	12.47	1.34	4.63	0.33
15	0.54	26.86	11.14	9.52	26.84	13.09	0.23	3.67	0.36

### Discussion

The SEM results show an elemental distribution map for thorium, cerium and neodymium with a homogenous distribution and no zonation present in the Steenkampskraal monazite. The presence of calcium (Ca<sup>+2</sup>) in the same sample (Fig 12) shows that it is possible for appetite Ca<sub>3</sub>(PO<sub>4</sub>)<sub>2</sub> with a similar structure to that of monazite to be present. However further analysis may reveal that the detected calcium in the elemental distribution (Fig 12) can be attributed to the presence of calcite or other carbonates in the monazite material. The presence of calcium in the sample indicates that the monazite material obtained is not 100 % concentrated.

The MPA analysis shows an average of 6.5 wt. % thorium as oxide over the 15 chosen analysis points. The average MPA concentrations for cerium and neodymium were 24.1 wt. % and 9.7 wt. % respectively.

<sup>24</sup> For analysis report of the minor elements see Appendix B.

**Table 8 Average weight % of Th, Ce and Nd in Steenkampskraal monazite  
(expressed as wt. % element oxide)**

Element	Average	STDev <sup>25</sup>
ThO <sub>2</sub>	6.5	1.2
Ce <sub>2</sub> O <sub>3</sub>	24.1	1.3
Nd <sub>2</sub> O <sub>3</sub>	9.7	0.3
La <sub>2</sub> O <sub>3</sub>	11.2	0.5

Table 8 shows the average oxide weight percentages of the most important elements to this study obtained from the MPA point analysis method. This table also shows the standard deviation of these concentrations as obtained from Table 7. A relatively low deviation for the lanthanides is observed with an increase in variance for thorium. This variance may be explained due to the variation in the intra-grain concentration between grains, while the concentrations for each grain were relatively uniform. It is of interest to note as the thorium concentration decreases a corresponding increase in cerium concentration was measured confirming the presence of varying solid solution in the monazite in this deposit.

Using the data represented in Table 7 and trace element concentrations of the same material in Appendix B (Table 17) an empirical formula<sup>26</sup> is calculated to consist of (Ce<sub>0.2</sub>,La<sub>0.1</sub>,Nd<sub>0.1</sub>,Th<sub>0.03</sub>,X<sub>0.07</sub>)PO<sub>4</sub> with X representing other minor oxides present in the sample. The theoretical empirical formula from Gaines *et al.* (1997) is given as (Ce<sub>0.5</sub>,La<sub>0.25</sub>,Nd<sub>0.2</sub>,Th<sub>0.05</sub>)PO<sub>4</sub>. In comparing these two formulas the difference in the calculated value compared to the theoretical value is explained in terms of the theoretical formula assuming that the monazite only consists of Ce, La, Nd, and Th as constituting REE's. The MPA analysis therefore was probably not inclusive of other elements such as Ga.

<sup>25</sup> Standard deviation calculated

<sup>26</sup> Detail for calculations explained in Appendix B

### 3.2 Extraction equipment

The LECO TFE 2000™ was utilized as the supercritical extractor of which in this section some of the key subsystems are described. A description and measures taken to solve problems encountered during operations is presented in detail in Appendix A. These problems encountered with the machine operation required considerable input and an engineering approach to solve. Figure 14 presents an illustration of the LECO TFE 2000™ employed with the attached modifier unit on the right hand side namely the M2000 modifier unit with some additional key subsystems such as the extraction chamber, collection chamber and thimble holders.



**Figure 14 LECO TFE 2000™ supercritical extraction apparatus and set-up**

The major subsystems shown in Figure 14 include the extraction chamber, the collection system and thimble holder. The use each of these components is explained in the flow diagram presented in Section 2.4. Other major components not shown in Figure 14 include the pump and variable restrictors which are described and considered in detail in Appendix A.

### 3.3 SFE extraction procedure

The procedure described in this section was used for each of the extraction principles applied or researched and is inclusive of the sample preparation, loading of samples and subsequent extractant preparation for chemical analysis.

In each of the proposed extractions the solid samples were carefully weighed and appropriate masses of the sample (0.25 g of monazite for thorium extraction and 0.5 g of as received crushed marula seed for the validation of the modified apparatus) were added to the thimbles.

A 0.2 M TBP-methanol solution was prepared and placed in the M2000 modifier unit. This solution served as the co-solvent for all subsequent extractions unless otherwise stated.

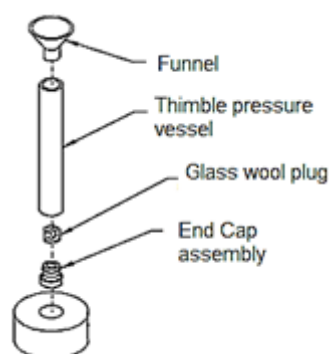


**Figure 15 Exploded view of the sample holder assembly including a funnel  
(LECO TFE 2000™ manual)**

The sample were loaded according to the schematic represented in Figure 15 with glass wool plugs added above and below the sample in conjunction with the fitted stainless steel filters (Appendix A) to prevent accidental flushing of the host sample from the extraction cell. Next glass wool and 10 mL methanol was additionally added to the collection vials to form an inert solid trap as described in Section 2.7.

Subsequently the thimbles were placed inside the extraction chamber followed by manual starting of the extraction procedure using the specific extraction conditions set forth by each experiment in Sections 3.4, 3.5 and 3.6.

After the extraction time had elapsed the system was depressurized by a continuous flow extraction protocol; without adding co-solvent or chelate to the extraction chamber during this stage. Once the system had been completely depressurized the solute was retrieved from the glass vials attached to the collection system.

After an extraction was completed the glass wool from the collection vial was washed with 5 mL of methanol to ensure no extracted solute remained in the glass wool. Thereafter the 15 mL extracted solute-methanol solution was distilled to a 10 mL solution and subsequently diluted for ICP-MS analysis. The dilution of the sample was achieved by using 9.9 mL of a 2 % HNO<sub>3</sub> solution and adding 0.1 mL of the extracted solute-methanol solution. The prepared samples were then used for ICP-MS analysis. The solid sample remaining in the thimble after extraction was removed and washed from the glass wool plugs with 10 mL of methanol. These samples were subsequently dried and used for XRF analysis.

Finally the effectiveness of extracting Th from filter paper was investigated in order to be able to calculate the SFE efficiency obtained during the thorium from filter paper extractions. The extraction was done by loading 3 mL of ICP standard Th(NO<sub>3</sub>)<sub>4</sub> solution onto filter paper and subsequent drying. Thereafter the Th(NO<sub>3</sub>)<sub>4</sub> was washed from the two samples with 10 mL methanol. The washing of the thorium nitrate from the filter paper was achieved by placing the filter paper inside a glass vial with the methanol and shaking the vial vigorously. This solution was then diluted using the same method as above and sent for ICP-MS analysis. All SF extractions were done in triplicate to ensure repeatability.

The following procedure was used to ensure no cross contamination between subsequent extractions.

- Before each new set of extractions the system was set to Helium purge for 10 min.
- The system was primed before each new set of extractions to ensure no unwanted gasses were trapped in the operating cycle.
- Each thimble and collection vial was washed in chromatographic grade methanol before each new extraction commenced.
- For each extraction new glass wool plugs were used along with 10 mL of chromatographic grade methanol.
- To further ensure no residual analytes were left in the extraction equipment a flushing protocol was used between each extraction; this protocol consisted of a blank extraction at the current extraction conditions.

### 3.4 Kumar experiment

In order to verify the extraction conditions and procedure for SFE extraction of thorium a similar SFE extraction procedure used by Kumar *et al.* (2009a) was reproduced.

The thorium used in this experiment was obtained from an ICP standard containing  $1000 \pm 3$   $\mu\text{g/mL}$   $\text{Th}(\text{NO}_3)_4$ . The ICP standard solution (3 mL) was dripped onto a filter paper and subsequently dried for 20 min. The dried sample was carefully inserted into the extraction vessel. The extraction conditions are presented in the Table 9.

**Table 9 Thorium filter paper extraction procedure conditions**

Variable:	Set point value:	Additional observations:
Pressure (bar)	200	
Temperature ( $^{\circ}\text{C}$ )	60	This temperature includes the HVR <sup>27</sup> temperature
Extraction time: (min)		
Static	20	
Dynamic	20	
CO <sub>2</sub> flow rate (ml/min)	2	
Co-solvent:	TBP-methanol	
Flow rate (ml/min)	0.2	

During this experiment an *in situ* complexation method was followed with 0.3 mL of TBP and HFA in a 1:1 volume ratio. Pressurization with a CO<sub>2</sub>, TBP-methanol 0.2 M solution was fed into the reaction vessel with a co-solvent rate of 0.2 mL/min.

<sup>27</sup> HVR's (heater variable restrictors) control the flow rate from the extraction vessel to the collection vial

*Results and discussion*

Table 10 contains three unique sets of results for the Kumar extraction namely the back extraction results as explained in Section 3.3, the results for samples taken from the collection vials and the results obtained through washing of the post-extraction samples.

**Table 10 Results for the Kumar experiment**

Sample	Concentration (mg/L)
Back extraction 1	2.12
Back extraction 2	3.36
Collection vial 1	<0.10
Collection vial 2	<0.10
Collection vial 3	<0.10
Extraction vessel 1	0.91
Extraction vessel 2	1.54
Extraction vessel 3	1.35

In order to validate the accuracy of the ICP-MS used to analyse these samples, two independent ICP-MS service providers were supplied with a sample containing the thorium standard. The concentrations of these test samples were unknown to the laboratories. The results obtained for the two independent ICP-MS analysis are shown in table 11.

**Table 11 Results of ICP-MS analysis for the thorium standard**

	( $\mu\text{g/mL}$ )
Standard	1000
ICP-MS 1	
Sample 1	15.87
Sample 2	13.23
ICP-MS 2	
Sample 1	15.69

From the results obtained a factor 100 difference in concentration is observed between the standard (supplied at concentration of 1000 µg/mL) and the two independent ICP-MS analysis reported in Table 11. This variation in concentration is explained in two ways:

- Firstly during ICP-MS analysis a dilution curve is produced by diluting the known standard to the approximate range of the expected results and thus calibrating the equipment. Subsequently the dilution curve in this range has a linear relation, however if the concentration is far above the expected range the linear relation may not hold producing errors in observed concentration.
- Secondly before the dilution curve was set-up an additional dilution was performed during which the standard was diluted 100 times, unfortunately this information was not supplied with the initial analysis.

Subsequently the results are discussed by accepting the standard to be of correct concentration.

From Table 10 the observed average concentration for the back extraction is calculated as 2.74 mg/L, with a theoretical maximum of 300 mg/L (after 10 mL methanol dilution from the leaching process) yielding a back extraction efficiency of 0.91 %.

The samples analysed from the collection vials in Table 10 showed no appreciable amounts of thorium collected. This may be an indicator that the trapping method used as described in Section 2.7 was ineffective.

The leached thorium from the post-extraction filter paper shows an average concentration of 1.27 mg/L. The overall extraction efficiency was then calculated by accepting 0.91 % leaching efficiency and 300 mg/L of available thorium before extraction; yielding an efficiency of 53 %

### 3.5 Ce substitution extraction protocol

In Section 2.4 the possibility of substitution of two ( $\text{Ce}^{+3}$ ) cations for a  $\text{Th}^{+4}$  cation in monazite was identified as a consequence of favourable crystal chemical considerations under supercritical fluid conditions. This section describes the procedure followed in exploring this option.

**Table 12 SFE  $\text{Ce}^{+3}$  substitution conditions**

Variable:	Set point value:	Additional observations:
Pressure (bar)	200	
Temperature ( $^{\circ}\text{C}$ )	60	This temperature includes the HVR <sup>28</sup> temperature
Extraction time: (min)		
Static	20	
Dynamic	20	
$\text{CO}_2$ flow rate (ml/min)	2	
Co-solvent:	TBP-methanol	
Flow rate (ml/min)	0.2	

- This experiment added chelates namely TBP and HFA *in situ* to the extraction before extraction commenced.
- 2ml of  $\text{Ce}(\text{NO}_3)_2$  at concentrations of 1mg/l was added *in situ* to each thimble (due to limitations in thimble size and availability of  $\text{Ce}(\text{NO}_3)_2$  ) resulting in hypo stoichiometric reaction conditions.
- The specific extraction conditions used during this experiment is listed in Table 12.

<sup>28</sup> HVR's (heater variable restrictors) control the flow rate from the extraction vessel to the collection vial

The effect temperature, pressure, grain size and extraction time had on the extraction efficiency in this procedure (Ce for Th) was investigated by employing a single variance experimental approach. In which the variables were kept constant and a single variable was chosen and varied to determine the influence of this variable on the extraction.

*Temperature variation*

The temperature variation study was initiated at 80 °C and increased in increments to a value of 150 °C.

*Pressure variation*

To investigate the influence pressure has on the extraction efficiencies the pressure of the extraction procedure was varied from an initial value of 200 bar to a maximum of 500 bar.

*Extraction time variation*

The effect extraction time has on the extraction efficiency was investigated by varying the extraction time from an initial 40 min static flow extraction time to 360 min static time. For each extraction the continuous flow extraction time was set to 10 min.

*Grain size variation*

To investigate the influence of the particle size and thus the surface area on the extraction efficiency, the grain size of each extraction material (monazite) was reduced starting with the initial value of 200 µm decreasing to a value of 38 µm. This decrease in particle size was achieved through grinding and sieving.

Eighty extractions were done to ensure all parameter variations discussed above were completely explored however, due to the cost involved with the XRF (X-Ray fluorescence spectroscopy) analysis of these samples it was decided to only analyse the  $\alpha$  and  $\beta$  substitution extractions considered next.

### 3.5.1 Ce<sup>+3</sup> substitution $\alpha$ -extraction procedure

The same extraction procedure and conditions outlined in Section 3.5 was used however the  $\alpha$  substitution extractions employed both TBP and HFA (0.3 mL) as chelates which were added *in situ* to the extraction vessel in a 1:1 volume ratio.

#### *Results and discussion for the $\alpha$ -extraction*

Table 13 shows the concentration of thorium oxide expressed as a weight % obtained through the  $\alpha$ -extraction procedure. It should be noted that the oxide was calculated using a +4 oxidation state for thorium in the XRF analysis.

**Table 13 Ce<sup>+3</sup>  $\alpha$ -extraction protocol ThO<sub>2</sub> concentration  
(XRF analysis)**

Sample	ThO <sub>2</sub> wt. %
1	6.8
2	6.9
3	6.6

Using the data represented in Table 13 the average thorium content as thorium oxide for the  $\alpha$ -extraction procedure is 6.8 wt. %. Comparing this value with the average of 6.5 wt. % thorium oxide obtained from the MPA analysis and considering a given 10 % error in the XRF analysis the percentage of extracted Th for this experiment appears negligible. The error margin stated was supplied by the analytical laboratory responsible for the analysis. For the extraction to have shown that thorium was indeed extracted the values in Table 13 should have been at least 10 % lower than the average thorium content before extraction commenced.

In Section 2.4.2 the general substitution suggested for the Ce<sup>+3</sup> and Th<sup>+4</sup> requires two cerium atoms for each thorium to be substituted. This extraction utilized 0.25 g of monazite sample per extraction chamber with an average of 6.5 wt. % thorium content yielding 0.016 g of thorium available for extraction. The 2 mL of cerium solution used in the substitution is of 1000  $\mu$ g/mL concentration. From the concentration values of both thorium and cerium it is clear the limiting factor in the reaction is the availability of cerium ions. With the reaction and limiting concentration of cerium now known it is possible to calculate the theoretical maximum extraction efficiency obtainable under the conditions set forth in Section 2.4.2 and is found to be 12 %

### 3.5.2 Ce<sup>+3</sup> substitution $\beta$ extraction procedure

The  $\beta$  extraction was carried out by using the same SFE extraction conditions as listed in Table 12 however only 0.3 mL of TBP as chelate was added *in situ* to the extraction vessel. The remaining extraction protocol followed the same procedure as the  $\alpha$ -extraction protocol.

#### *Results and discussion for the $\beta$ -extraction*

Table 14 shows the thorium oxide weight percentages obtained through XRF analysis of the materials extracted according to the  $\beta$  extraction protocol.

**Table 14 Ce<sup>+3</sup>  $\beta$ -extraction protocol ThO<sub>2</sub> concentration**

Sample	ThO <sub>2</sub> wt. %
1	7.2
2	7.5
3	7.4

From the data represented in Table 14 it is calculated that the average weight percentage for thorium expresses as thorium oxide in the  $\beta$  extraction is 7.4 wt. %.

Comparing the average values for Table 13 and Table 14 a 0.6 wt. % difference in average thorium oxide content was obtained through the two procedures followed. This variation in thorium content may be attributed to the 10 % error margin produced during the XRF analysis method. From the results for both  $\alpha$  and  $\beta$  substitution extraction it is clear the extraction efficiency is below the XRF analysis method error range. These results gave rise to a study to validate the operational effectiveness of the extraction equipment.

### 3.6 Ce<sup>+3</sup> Extraction validation

The validation of the repair and modification to the LECO TFE 2000™ operational conditions and effectiveness was conducted through the extraction of *Sclerocarya birrea*<sup>29</sup> seed oils from solid seeds. The results of which was compared with the extraction weight obtained on a similar material using a fully operational certified pilot plant dedicated to seed oil extraction of *Sclerocarya birrea*. The mass difference was calculated on a gravimetric basis with the conditions of the extraction shown in Table 15.

**Table 15 Marula seed oil extraction procedure conditions**

Variable:	Set point value:	Additional observations:
Pressure (bar)	200	
Temperature (°C)	60	This temperature includes the HVR temperature
Extraction time: (min)		
Static	40	
Continuous	10	
CO <sub>2</sub> flow rate (ml/min)	2	
Co-solvent:	None	
Flow rate (ml/min)	-	

A mass of 0.5 g crushed marula seed was added to each thimble and re-weighed to ensure no errors were made during transfer from the glass vial used for measuring.

After the extraction was completed the thimbles containing the marula seeds were re-weighed and the difference in weight calculated. The difference in weight obtained was then compared with another independent SF extractor (Fig 16) of the Bio Beneficiary Group of the North-West University to validate the experimental setup.

<sup>29</sup> *Sclerocarya birrea* commonly known as the Marula tree



**Figure 16 NATEX SFE pilot plant used for validation of marula oil extraction.**

*Results and discussion*

Table 16 shows the results obtained from extracting marula seed oil. The extraction efficiency was calculated on a gravimetric basis.

**Table 16 Marula seed oil extraction weight**

Sample	Pre-extraction mass (g)	Post-extraction mass (g)
1	0.58	0.30
2	0.55	0.27
3	0.53	0.27

From the data in Table 16 the average weight difference is calculated as 50 wt. %. This value was correlated with the independent SFE extractor at the North-West University and found to be similar.

## 4 Conclusion

In this chapter conclusions are drawn regarding the feasibility of thorium extraction from monazite using a SFE process with various chelates. The SFE extraction process draws from a review of solvent extraction procedures dictating the necessity for correct solvent, co-solvent and chelate choice. Furthermore, conclusions are drawn on the feasibility of a substitution mechanism for the SFE extractions.

From the SEM and subsequent MPA analysis of Steenkampskraal monazite the conclusion is made that the concentration of thorium available in the monazite is an average of 6.5 weight %. Furthermore, the distribution of thorium within the monazite grains is homogeneous although zonation may be present in other mineral composites therefore affecting the obtainable efficiencies from those structures.

To verify the SFE procedure used for transition metals a notable SFE extraction procedure from literature was reproduced. The results of this extraction showed an efficiency of 53% compared with the results from literature of 83 %. Due to the ineffectiveness of inert solid trapping methods revealed during this experiment all subsequent extracted samples from monazite were tested by XRF powder analysis methods.

The proposed crystal chemical substitution of  $Ce^{+3}$  for  $Th^{+4}$  allowed from theory and confirmed in literature was investigated using a SFE process. From this extraction it is concluded that the extraction efficiency of thorium was below the laboratory supplied error limit of 10 % for the XRF powder analysis method. From the results obtained for the  $\alpha$  and  $\beta$  cation substitution extractions it is of interest to note the average thorium oxide content in the  $\beta$  extraction was 7.4 wt % which employed only TBP in an *in situ* extraction process. This concentration appears slightly higher than the  $\alpha$  extraction average concentration of 6.8 wt %. The  $\alpha$  extraction used both a TBP and HFA chelate in a synergistic *in situ* extraction process. Whether this variation is due to errors in the analysis method or possible success of extraction is unknown. It is therefore recommended that the extraction be repeated at higher concentrations of  $Ce^{+3}$  available for substitution.

Before and during experimental work the extraction apparatus was plagued by continual technical breakdowns due to prior work by other users. These problems stemmed primarily from lack of proper support by the suppliers and poor extraction protocols by previous users. In each case the problem was examined and solved from a mechanical engineering standpoint.

In order to verify the effectiveness of the modified apparatus, marula seed oil from marula seeds were extracted and the results obtained compared with an independent SFE extraction apparatus. The obtained results show an extraction efficiency of 50 wt. % for each of the two independent apparatus.

Finally, from the literature a method for the substitution of trivalent cations for tetravalent cations in a monazite structure has been shown. The experimental implementation of this substitution was unsuccessful possibly due to a low theoretical extraction limit of 12 % coupled with the supplied error limit of 10 % produced during the XRF analysis.

It is recommended that in order to further improve the extraction efficiency of thorium from monazite the (Ce<sup>+3</sup>) substitution extraction be repeated using longer extraction times to allow for complete diffusion into and from the sample structure. Furthermore extractions using a more concentrated fluorinated chelates may be of value due to the abundance of work from literature showing the effectiveness of fluorinated ligands.

## 5 Bibliography

- Clavier, N., Podor, R. & Dacheux, N. 2011. Crystal chemistry of the monazite structure. *J. Eur. Ceram. Soc*, 31:941-976.
- Cornelius, S., Hurlbut, J. & Cornelius, K. 1977. Manual of Mineralogy (after J.D. Dana).
- Darr, J.A. & Poliakoff, M. 1999. New direction in inorganic and metal-organic coordination chemistry in supercritical fluids. *Chem. Rev.*, 99:495-541.
- Davis, J.B., Marshall, D.B., Oka, K.S., Housley, R.M. & Morgan, P.E.D. 1999. Ceramic composites for thermal protection systems. *Comp. part A*, 30:483-488.
- Dean, J.R. 1993. Applications of supercritical fluids in industrial analysis. NewCastle: Blackie Academic & Professional, an imprint of Chapman & Hall.
- Gaines, Richard, V., Skinner, H., Catherine, W., Foord, E.E., Mason, B. & Rosenzweig, A. 1997. Dana's New Mineralogy. Eighth edition. New York: John Wiley & Sons, Inc.
- Gaudernack, B., Hannestad, G. & Hundere, I. 1971. United States. Patent No C22B59/00, C01F17/00.
- Ghoreishi, S.M., Ansari, K. & Ghazaikar, H.S. 2012. Supercritical extraction of toxic heavy metals from aqueous waste via Cyanex 301 as chelating agent. *The J. Supercrit. Fluid.*, 72:288-297.
- Herbst, R.S., Baron, P. & Nilsson, M. 2011. Standard and advanced separation: PUREX processes for nuclear fuel reprocessing. (In Nash, K.L. & Lumetta G.J., eds. Advance separation techniques for nuclear fuel processing and radioactive waste treatment. 1st Edition: Woodhead publishing.
- Herrero, M., Mendiola, J.A., Cifuentes, A. & Ibanez, E. 2010. Supercritical fluid extraction: Recent advances and applications. *J. Chromat. A*, 1217:2495-2511.
- Kamlet, M.J., Abboud, J.-I.M., Abraham, M.H. & Taft, R.W. 1983. Linear solvating energy relationships 23. A Comprehensive collection of the Solvatochromic parameters  $\pi$ ,  $\alpha$  and  $\beta$  and some methods for simplifying the generalized solvatochromic equation. *J. Org. Chem*, 48:2877-2887.
- King, J.W. & Friedrich, J.P. 1990. Quantitative correlations between solute molecular structure and solubility in supercritical fluids. *J. Chromat*, 517:449-458.
- Kumar, P., Rao, A. & Ramakumar, K.L. 2009a. Supercritical fluid extraction of uranium and thorium from liquid and solid matrices. *Radiochim. Acta*, 97:105-112.
- Laintz, K.E. & Wai, C.M. 1992. Extraction of Metal Ions from liquid and Solid Materials by Supercritical Carbon Dioxide. *Anal. Chem*, 64, 2875-2878.

- Lin, Y., Brauer, R.D., Laintz, K.E. & Wai, C.M. 1993. Supercritical Fluid Extraction of Lanthanides and Actinides from Solid Materials with a Fluorinated B-diketone. *Anal. Chem.*, 65:2549-2551.
- Lin, Y., Smart, N.G. & Wai, C.M. 1995. Supercritical Fluid Extraction of Uranium and Thorium from Nitric Acid Solutions with Organophosphorus Reagents. *Environ. Sci. Technol.*, 29 (10):2706-2708.
- Lin, Y. & Wai, C.M. 1994. Supercritical Fluid Extraction of lanthanides with fluorinated B-diketones and tributyl phosphate. *Anal. Chem.*, 66:1971-1975.
- Lin, Y., Wai, C.M., Jean, F.M. & Brauer, R.D. 1994. Supercritical Fluid Extraction of Thorium and Uranium Ions from Solid and Liquid Materials with Fluorinated B-diketones and Tributyl Phosphate. *Environ. Sci. Technol.*, 28:1190-1193.
- Luque de Castro, M.D. & Priego-Capote, F. 2010. Soxhlet extraction: Past present panacea. *J. Chromat. A*, 1217:2383-2389.
- Montel, J.M., Glorieux, B., Seudoux-Guillaume, A.-M. & Wirth, R. 2006. Synthesis and sintering of a monazite-brabantite solid solution ceramic for nuclear waste storage. *J. Phys. Chem. Solids.*, 67:2489-2500.
- Ni, Y., Hughes, J.M. & Mariano, A.N. 1995. Crystal Chemistry of monazite and Xenotime structures. *Am. Mineral.*, 80:21-26.
- Podor, R. & Cuney, M. 1997. Experimental study of Th-bearing LaPO<sub>4</sub> (780 °C, 200 MPa): Implications for monazite and actinide orthophosphate stability. *Am. Mineral.*, 82:765-771.
- Rao, A., Kumar, P. & Ramakumar, K.L. 2010. Separation of uranium from different uranium oxide matrices employing supercritical carbon dioxide extraction. *J. Radioanal. Nucl. Chem.*, 285:247-257.
- Shamsipur, M., Ghaisvand, A.R. & Yamini, Y. 2001. Extraction of uranium from solid matrices using modified supercritical fluid CO<sub>2</sub>. *J. Supercrit. Fluid.*, 20:163-169.
- Song, W.-S., Choi, H.-N., Kim, Y.-S. & Yang, H. 2010. Formation of green-emitting LaPO<sub>4</sub>:Ce, Tb nanophosphor layers and its application to highly transparent plasam displays. *J. Mater. Chem.*, 20:6929-6934.
- Taylor, L.T. 1996. Supercritical Fluid extraction. A Wiley-Interscience publication.
- Terra, O., Dacheux, N., Clavier, N., Podor, R. & Audubert, F. 2008. Preparation of optimized uranium and thorium bearing brabantite or monazite/brabantite solid solutions. *J. Am. Ceram. Soc.*, 91 (11):3673-3682.
- Wai, C.M. & Wang, S. 1997. Supercritical fluid extraction: metals as complexes. *J. Chromat.*, 785:369-383.
- Xie, F., Zhang, T.A., Dreisinger, D. & Doyle, F. 2014. A critical review on solvent extraction of rare earths from aqueous solutions. *Minerals Engineering*, 56:10-28.

- (1) Accesed 10/10/14 [http://chemwiki.ucdavis.edu/wikitexts/US\\_Davis/UCD\\_Chem\\_2B/UCD\\_Chem\\_2B%3A\\_Larsen/Unit\\_II%3A\\_States\\_of\\_Matter/Intermolecular\\_Interactions/11.7\\_Phase\\_Diagrams](http://chemwiki.ucdavis.edu/wikitexts/US_Davis/UCD_Chem_2B/UCD_Chem_2B%3A_Larsen/Unit_II%3A_States_of_Matter/Intermolecular_Interactions/11.7_Phase_Diagrams)

## 6 Appendix A: Extraction equipment

### 6.1 Major subsystems

This section focuses on the supercritical extractor discussing the major subsystems in order to assist the reader in understanding the operation and modifications made to the LECO TFE 2000™ extractor during the course of this study.

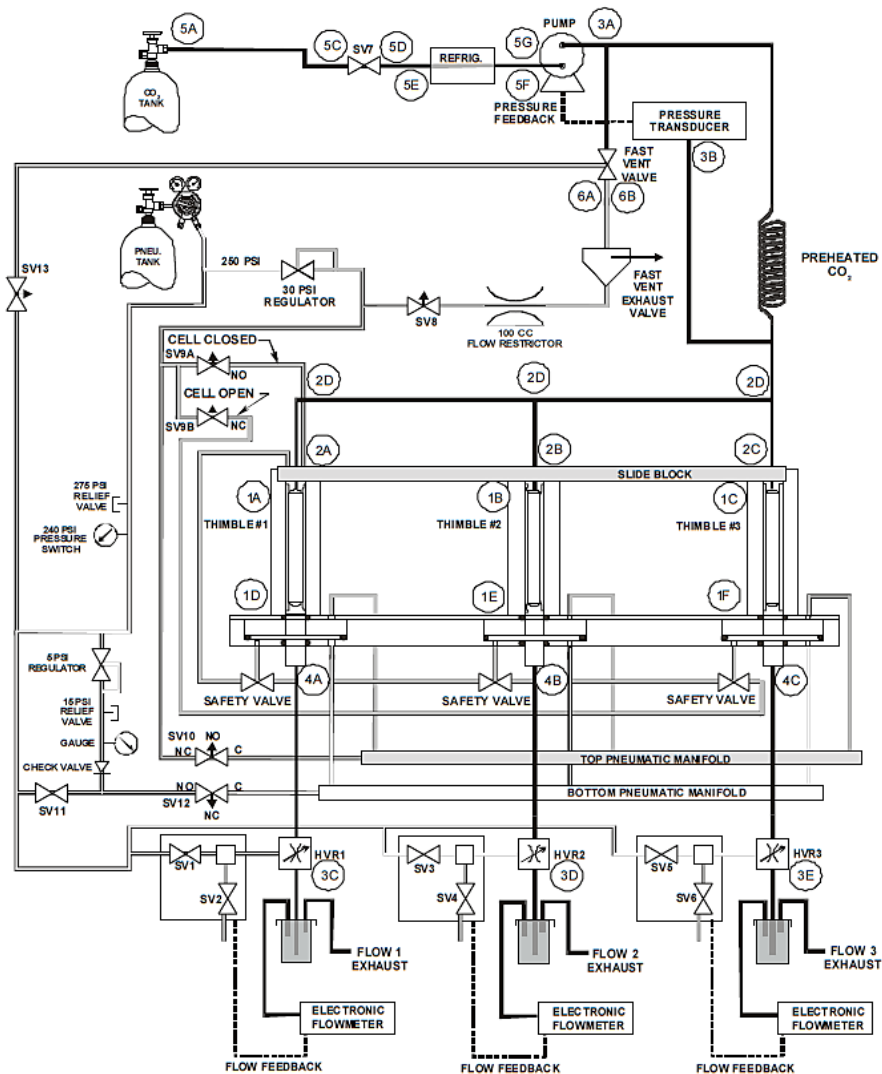


**Figure 17 Schematic flow diagram of the LECO TFE 2000™**

Figure 17 presents a schematic flow diagram of all the major components in the LECO TFE 2000™ extractor. This diagram was obtained from the LECO TFE 2000™ manual.

*Extraction vessel*

The extraction vessel is fitted with two frits<sup>30</sup> located in the frit cap to ensure no flushing of the host sample during the extraction process. The LECO TFE 2000 furthermore uses 3 extraction vessels each with a volume of 10ml that can safely handle pressures up to 620 atm. The location of these extraction vessels in the flow diagram (Fig 17) are shown as 1A, 1B and 1C. Figure 18 shows each component of the thimble vessel and illustrates how these components are fitted together to form an assembled thimble. The seals shown in Figure 18 are radial spring energized seals the replacement of which due to wear is discussed in Section 6.1.1.

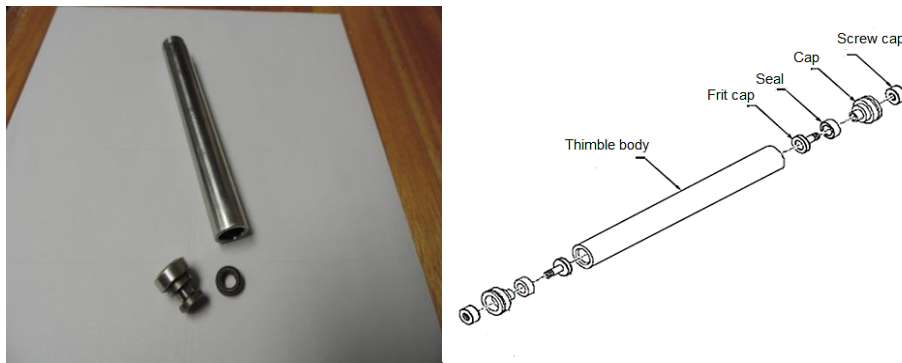


**Figure 18 A photo (left) and an exploded view of the thimble vessel assembly  
(LECO TFE 2000™ manual)**

Figure 19 shows a scanning electron microscope image of the stainless steel filter (frit) found in the LECO TFE 2000 as seen at different magnifications.

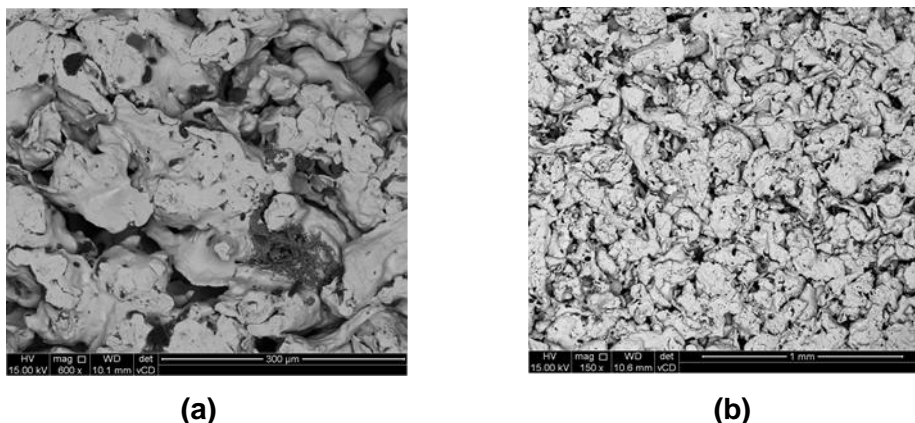


**Figure 19 Photo of the porous stainless steel filter (a) 600x magnification  
(b) 150x magnification**

<sup>30</sup> Frits refer to a porous stainless steel waver as shown under magnification in figure 17.

### *Pump*

The LECO TFE 2000™ utilizes a reciprocating pump design capable of safely delivering pressure of up to 620 atm at a maximum flow rate of 4ml/min with the pump shown in Figure 17 as 5G and 5F.

### *Restrictor*

The LECO TFE 2000™ utilizes heated variable restrictors to regulate the flow and therefore to some degree the pressure from the extraction cell during the continuous flow extraction protocols used or during depressurization. The heated variable restrictor consists of several parts shown in Figure 19 and is operated by a pneumatic piston that exerts a force on the pin. The force exerted on the pin is translated to the needle pin which regulates the fluid flow rate.

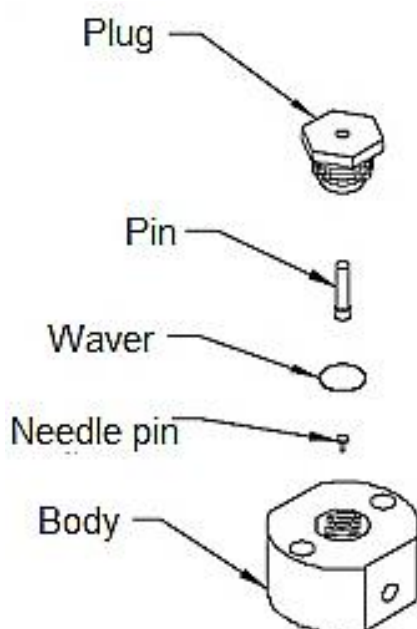


**Figure 20 Exploded view of a schematic for the variable restrictor**

**(LECO TFE 2000™ manual)**

Figure 20 shows an illustration of the assembly schematic for a variable restrictor assembly found in the LECO TFE 2000™ manual. The HVR's are located at 3C, 3D and 3E in Figure 17.

### **6.1.1 Engineering and maintenance of the LECO TFE 2000™**

The LECO TFE 2000™ was initially procured from the Department of Chemistry at the North West University but was found to be in need of extensive repair and maintenance during this research due to several problems listed below which were solved or attended to using an engineering approach.

#### *Poor maintenance and extraction protocols*

Initially after receiving the extraction apparatus it was evident that prior poor maintenance and extraction protocols led to the entire system being full of oily residue inhibiting proper operation. In order to correct this problem the entire extraction assembly was disassembled and each part individually cleaned. New O-rings were installed on all transfer tubing leading to and from the collection vessels. After cleaning, the LECO TFE 2000 was run several times in a blank extraction protocol to ensure no contaminants remained inside the system.

#### *Blockage in transfer tubing*

It was later found during initial extraction protocols that the 1/16" stainless steel transfer tubing from the extraction cell to the HVR's was blocked allowing only one of the three extraction channels to be used. These tubing were removed and placed in an ultrasonic bath overnight to ensure all possible contaminants and blockages were removed. After reconnecting the tubing an electronic CO<sub>2</sub> detector was acquired and used to detect and ensure no leakage occurred at any of the connections.

### *Extraction cell leakage*

Initially the LECO TFE 2000 was incapable of achieving and maintaining the set extraction pressures due to leakage in the radial thimble seals (Fig. 21). The cause of this leakage was attributed to wear and tear of the seals during every day normal previous operation. This problem was corrected by initially replacing the seals with new seals found during the procurement of the machine, however these seals were of incorrect size

and induced severe leakage at operating pressure. In order to successfully replace these seals a specialist company (Seal & Gasket) manufactured new spring energized radial thimble seals from PTFE 2 according to the author's specifications. These specifications for the seals were deduced from the worn seals accompanying the apparatus. The figure below shows an isometric view of the radial thimble seal with a cross sectional view to show hidden detail.

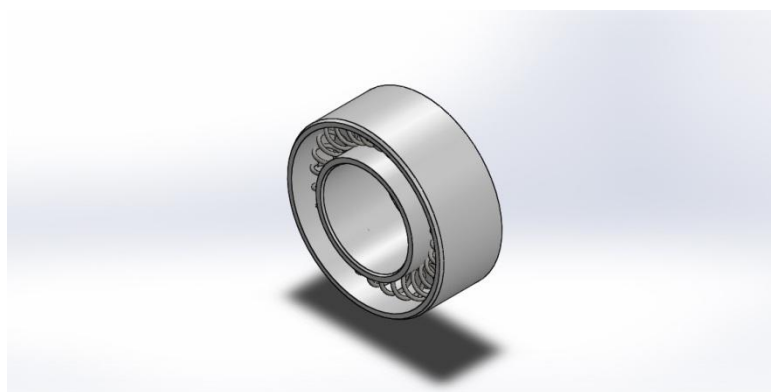


**Figure 21 Isometric view of a radial thimble seal model**

### *Leakage in the heated variable restrictors*

The heated variable restrictors (HVR) control the flow of solvent-solute complex from the extraction chamber to the collection vials. Leakage of the HVR's leads to poor results especially with regards to static flow extractions due to the reduction in contact time that the chelates spend with the host sample before being flushed from the extraction cell. Initially an attempt was made to repair the existing HVR's by manufacturing new stainless steel wavers as shown in Figure 19 and additional machining of the needle pin and body to ensure a gas tight metal seal. However after these modifications, a persistent leakage of roughly 0.1ml/min was still observed. To solve this problem three Series 410 high pressure needle valve's from Swagelok were procured and installed in the transfer tubing leading to the HVR's. The installation of these valves in front of the HVR's was to ensure that no freezing/blockage of the valves would occur during the rapid expansion of gas that takes place during continuous flow and decompressions protocols.

After successful installing the needle valves a new problem associated with regulating the flow through the system arose. This problem was caused by the lack of pressure on the HVR's during static flow extractions as a result of the installation of the needle valves and subsequent rapid addition of pressure during the continuous flow protocols. To overcome this problem the pneumatic control over the HVR's was completely disabled and three flow regulators were installed on the exhaust line of the collection vials to enable manual control of the flow through the system. This allowed for effective bypassing of flow control by the HVR's. However, flow control now shifted to the high pressure needle valves installed. To ensure these valves did not freeze during extractions they were immersed in a container filled with water and kept at a constant 20°C.



**Figure 22 The modified LECO TFE 2000**

Figure 22 shows the LECO TFE 2000 after modification were completed.

## 7 Appendix B: Data and calculations

This section shows the minor element concentrations associated with the MPA analysis positions presented in Table 7. Furthermore this section contains the calculations used to determine the empirical formula of the monazite presented in Section 4.

**Table 17 MPA of minor elements of Steenkampskraal monazite  
(wt. % as elemental oxide)**

ID	Dy <sub>2</sub> O <sub>3</sub>	Eu <sub>2</sub> O <sub>3</sub>	FeO	Gd <sub>2</sub> O <sub>3</sub>	PbO	Pr <sub>2</sub> O <sub>3</sub>	Sm <sub>2</sub> O <sub>3</sub>	Tb <sub>2</sub> O <sub>3</sub>	U <sub>2</sub> O <sub>3</sub>	ZrO <sub>2</sub>
1	0.46	-	-	0.65	0.41	2.48	1.52	0.16	0.19	-
2	0.55	-	-	0.73	0.31	2.56	1.44	0.07	0.18	-
3	0.48	0.11	-	0.66	0.38	2.52	1.44	0.08	0.23	-
4	0.51	-	-	0.68	0.27	2.5	1.48	0.15	0.18	-
5	0.55	0.12	-	0.73	0.4	2.46	1.49	0.13	0.18	-
6	0.5	0.1	-	0.51	0.3	2.57	1.41	0.11	-	-
7	0.48	0.13	0.04	0.56	0.37	2.51	1.36	0.13	-	0.09
8	0.45	0.12	-	0.49	0.37	2.55	1.32	0.08	-	0.09
9	0.25	-	0.2	0.63	0.18	2.84	1.63	0.15	-	0.09
10	0.19	-	-	0.46	0.28	2.48	1.41	0.14	-	0.09
11	0.34	-	-	0.64	0.18	2.73	1.48	0.12	-	0.09
12	0.31	-	0.9	0.71	0.23	2.61	1.48	0.14	-	-
13	0.33	-	0.05	0.4	0.26	2.49	1.41	0.07	-	0.12
14	0.21	0.12	0.25	0.58	-	2.53	1.49	0.07	-	-
15	0.22	0.12	0.1	0.3	-	2.42	1.35	0.13	-	-

The calculation of an empirical formula for Steenkampskraal monazite was carried out by following the procedure outlined by Cornelius *et al.* (1977) and explained below.

**Table 18 Recalculation of empirical formula from MPA analysis data**

Element	Molecular Weight	Weight % oxide	Molecular Proportion
Th <sub>2</sub> O <sub>3</sub>	232.04	6.5	0.03
Ce <sub>2</sub> O <sub>3</sub>	140.12	24.1	0.2
La <sub>2</sub> O <sub>3</sub>	138.91	11.2	0.1
Nd <sub>2</sub> O <sub>3</sub>	144.24	9.5	0.1
X	-	0.1	0.07

Table 18 shows the molecular weight, oxide wt % and molecular proportion used to determine the empirical formula. The molecular weight was obtained from a periodic table of elements. The weight % oxide was obtained from Table 7 and 17. Finally the molecular proportion is calculated by dividing the wt % oxide by the molecular weight. Where X represents the combined data of the minor elements represented in Table 17.